LUND UNIVERSITY
Faculty of Science

Near-local density approximation approach to one-dimensional lattice systems

Basheer Joudeh

Thesis submitted for the degree of Bachelor of Science
Project duration: 2 months

Supervised by Associate Professor Claudio Verdozzi

LUND
UNIVERSITY

Department of Physics
Division of Mathematical Physics
June 2018

Abstract

Describing many-body quantum systems has been an analytically and computationally challenging task since the advent of quantum mechanics. However, in the past 50 years as a result of our technological advancement and the emergence of methods such as density-functional theory (DFT), we have taken crucial steps forward regarding our ability to study and understand large quantum systems. In this work, we have studied the extended Hubbard model using a mean-field approximation where we have tested an approach to the long-ranged electronic interaction that is not entirely local. We have developed a near-local approximation (NLA) for the model under study, where the exact non-local electronic interaction at site i is approximated using the densities at a pair of sites neighbouring i in addition to the density at i. As preliminary to a discussion of NLA, we showed results for the density of states of systems with a three-site supercell, thus providing a simple characterization of the mean-field treatment (in the case of local interactions only). When it comes to the main results of our work, i.e. a derivation and the testing of the NLA, our findings can be summarised as follows: we have found three NLA variants, namely a left site approximation (LSA), a right site approximation (RSA) and a center site approximation (CSA). Furthermore, we have found that CSA performs better than a local approximation both under the effect of a parabolic external potential and a distorted one. We have also found that the performance of LSA and RSA are scarce in general. Albeit this work (being based on the extended Hubbard model under a mean-field approximation) does not address exchange and correlation effects directly, it provides a first step towards future work where a near-local treatment is carried out on more accurate grounds.

Contents

Abstract i

Contents ii

Acknowledgments iv

Acronyms v

1 Introduction 1
- 1.1 Motivation . . . 1
- 1.2 Density-functional theory . . . 2
- 1.3 Scope of this work . . . 7

2 Theory 8
- 2.1 The Hartree-Fock approximation: A closer look . . . 8
- 2.2 Density-functionalising Hartree-Fock: The Hartree-Fock approximation for the extended Hubbard model . . . 9
- 2.3 Long-ranged interaction: A local approximation within Hartree-Fock . . . 12
- 2.4 Long-ranged interaction: A near-local approximation within Hartree-Fock . . . 12
- 2.5 A characterization of the Hartree-Fock solution via the density of states . . . 15

3 Results 17
- 3.1 Local density of states . . . 17
- 3.2 Performance of NLA . . . 19

4 Conclusions and Outlook 23

References 24

A Notation 26

B Derivations 27
- A derivation of Approximation 2: Additional details . . . 27
- A derivation of Equation (2.25) . . . 30
- A derivation of Statement 1 . . . 31
- A derivation of Statement 3 . . . 35

C Further Results: DoS 37

To my family back in Gaza.

Acknowledgments

I would like to express my sincerest gratitude to my supervisor and mentor Professor Claudio Verdozzi for introducing me to the research area of this thesis from scratch, for his patience when I took my time to learn the ropes, for verifying or correcting my code whenever I was in doubt and for being *always* available for memorable discussions. Thank you for allowing me to work under your supervision.

I would also like to thank Emil Boström for reading the manuscript and providing helpful comments. Furthermore, I would like to thank my brother Hamdi for his endless support, for assisting me with LaTeX and MATLAB and for being there whenever I needed help. Finally, I would like to thank my parents for their many sacrifices and never-ending support.

Acronyms

HF	Hartree-Fock
GS	Ground State
LDA	Local Density Approximation
DFT	Density-Functional Theory
HK	Hohenberg-Kohn
KS	Kohn-Sham
SOFT	Site-Occupation-Functional Theory
BALDA	Bethe-Ansatz Local Density Approximation
RHF	Restricted Hartree-Fock
LHFA	Local Hartree-Fock Approximation
NLA	Near-Local Approximation
LSA	Left Site Approximation
CSA	Center Site Approximation
RSA	Right Site Approximation
DoS	Density of States

Chapter 1

Introduction

1.1 Motivation

Following the mathematical formulation of quantum mechanics (1925-1930), physicists have been relentlessly on the search for a practical framework in which the theory can be used to study many-body systems. Although quantum mechanics is an exact theory for non-relativistic systems, the lack of computational means and the complexity of realistic systems made an application of the theory to large ensembles of particles a daunting task. One of the most prominent methods introduced during those years is the Hartree-Fock (HF) method. Strictly speaking, D. Hartree introduced the Hartree method in 1927 as a way of providing a mean-field approximation to describe electrons in atoms that fits into the picture of the emerging wave mechanics formalism [14]. A significant flaw in Hartree's initial formulation is that the method neglects the fermionic nature of electrons. The proposed equation by Hartree does not take into account the Pauli exclusion principle which was later corrected following the contributions of J. C. Slater, J. A. Gaunt and V. A. Fock [16–18]. By the year 1935, we had what is known as the Hartree-Fock (HF) method which takes into account the anti-symmetry of the wave-function of a fermionic system and can be viewed as a correction to the preceding Hartree method [15]. The HF method will act as a basis for the work presented in this thesis.

The Hartree-Fock method is a wave-function based approximative treatment of many-body quantum mechanical systems, which depends explicitly on the many-body wave-function of the system in question. In its simplest form, the HF method is a ground state (GS) stationary theory. The GS wave-function of a fermionic quantum mechanical system is approximated by a Slater determinant and the GS energy is calculated by invoking the variational principle, i.e. optimizing the expectation value of the energy with respect to the wave-function. Therefore, we have the following[1]:

$$\Psi_0 \approx \Phi_{\text{SD}} = \frac{1}{\sqrt{N!}} \det\{\aleph_1(\mathbf{x}_1)\aleph_2(\mathbf{x}_2)\cdots\aleph_N(\mathbf{x}_N)\} \tag{1.1}$$

$$\aleph_k(\mathbf{x}_i) = \phi_k(\mathbf{r}_i)\sigma(s_i) \tag{1.2}$$

$$E_0 \approx E_{\text{HF}} = \min_{\Phi_{\text{SD}}} E[\Phi_{\text{SD}}] \tag{1.3}$$

where N is the number of electrons in the system, $\{\aleph_j\}_{j=1}^{N}$ are spin orbitals consisting of a spatial part ϕ and a spin part $\sigma \in \{\uparrow, \downarrow\}$ and the energy functional $E[\Phi_{\text{SD}}]$ will be specified in the next chapter. The HF method approximates the ground state energy E_0 by finding the *optimal* Slater determinant that minimizes the energy functional $E[\Phi_{\text{SD}}]$.

[1] The notation adapted throughout this thesis is explained in Appendix A.

The HF method takes into account the quantum mechanical nature of the problem by invoking appropriate symmetry constraints on the approximated wave-function (Slater determinants being anti-symmetric abides by the Pauli exclusion principle for fermions). An immediate consequence of such constraint is a *non-local* energy term in the full solution called the *exchange* energy. That is, the solution can be written as:

$$E_{\text{HF}} = E_{\text{HF}} - E_x + E_x = \underbrace{E_l}_{\text{local}} + \underbrace{E_x}_{\text{non-local}} \tag{1.4}$$

where E_x is the exchange energy. The non-locality of E_x makes an exact calculation, more often than not, not achievable. An approximation for E_x can be obtained in the spirit of a *local density approximation* (LDA) or equivalently, by the *Hartree-Fock-Slater* method where the exchange hole is assumed to be spherically symmetric and centered around the electron. Formally, the exchange hole is defined as the difference between the conditional probability of finding an electron with spin σ at $\mathbf{r}_2$ given that a reference electron with the same spin is at $\mathbf{r}_1$, and the completely uncorrelated probability of finding an electron with spin σ at $\mathbf{r}_2$. It can be pictured as the reference electron digging a hole around it that results in repelling other electrons of the same spin due to the anti-symmetry of the total wave-function. Slater's approximation, which is in agreement with that of LDA, is given by [24]:

$$E_x[\rho] \approx E_x^{\text{Slater}}[\rho] = -\frac{9}{8}\left(\frac{3}{\pi}\right)^{1/3} \alpha_S \int \rho(\mathbf{r})^{4/3} d\mathbf{r} \tag{1.5}$$

where α_S is a semi-empirical factor between 2/3 and 1 and ρ is the electronic density. This approximation only requires the knowledge of the electronic density distribution of the system under study. Furthermore, equation (1.5) is local and significantly easier to employ than a non-local expression. In the same sense, the work presented in this thesis combines density-functional theory (DFT) and the HF method in order to obtain an approximation for non-local interactions (analogous to E_x) that is not entirely local, and compares it to a local one. However, this is targeted towards a different class of systems, namely lattice models. In particular, we focus on the Hubbard model [13].

1.2 Density-functional theory

An inevitable consequence of a pure HF treatment, which is in fact an approximation method, is a deviation away from the actual ground state energy in question. That is, the real problem can not be described by a single Slater determinant. This simplification leads to an error in estimating E_0. A single Slater determinant description often leads to *"electrons getting too close to each other"* [5, Ch. 1]. This is evident in the Hartree-Fock equations where the Coulomb repulsion part of the HF potential is taken into account only in average as we shall see in the next chapter. The difference between the HF energy and the exact ground state energy is what was initially granted the term

correlation energy, that is:

$$E_{\text{corr}} = E_0 - E_{\text{HF}} \tag{1.6}$$

which indicates that there is still plenty of room for improvement. Many approaches were taken to rectify this error with some being an extension to the original HF method, e.g. one can have a linear mixing of a very large number of Slater determinants called *configuration interaction* [19, Ch. 4]. However, one of the most effective and astonishingly easy to grasp approaches has its genesis in 1964, from the hands of P. Hohenberg and W. Kohn (HK).

In the 1950s, by the time digital electronic computers became available, the HF method was put to practice and this area of research became increasingly popular in numerical applications. The emergence of post-HF methods and DFT followed (and continues to) by the end of 1964. DFT has its roots in the HK seminal paper in 1964 where they provided the proof for two landmark theorems [1]. The *first HK theorem* states that: the external potential $V_{\text{ext}}(\mathbf{r})$ is a unique functional of the ground state density $\rho_0(\mathbf{r})$ up to a constant. It follows that the GS wave-function Ψ_0 is also a functional of $\rho_0(\mathbf{r})$ up to a multiplication by an arbitrary phase. For a Hamiltonian on the form:

$$\hat{H} = \hat{T} + \hat{U} + \hat{V}_{\text{ext}} \tag{1.7}$$

where $\hat{T}$ and $\hat{U}$ are the operators for the kinetic energy and the inter-particle interaction respectively, we can define the universal functional given by:

$$F[\rho_0(\mathbf{r})] \equiv \langle \Psi_0 | \hat{T} + \hat{U} | \Psi_0 \rangle. \tag{1.8}$$

The GS energy functional is then defined as:

$$E_{V_{\text{ext}}}[\rho_0(\mathbf{r})] \equiv F[\rho_0(\mathbf{r})] + \int V_{\text{ext}}(\mathbf{r}) \rho_0(\mathbf{r}) d\mathbf{r} \tag{1.9}$$

where the density can be expressed as the variational derivative of the energy with respect to the external potential. The *second HK theorem* states that: the total energy is minimized at the exact ground state density $\rho_0(\mathbf{r})$. The problem is then reduced to an optimization problem with respect to the density $\rho(\mathbf{r})$, that is:

$$E_0 = E_{V_{\text{ext}}}[\rho_0(\mathbf{r})] = \min_{\rho} \left(F[\rho(\mathbf{r})] + \int V_{\text{ext}}(\mathbf{r}) \rho(\mathbf{r}) d\mathbf{r} \right). \tag{1.10}$$

However, this does not provide us with any means of solving the problem or lower its complexity, albeit it does reformulate the problem in terms of the density $\rho(\mathbf{r})$ instead of the wave-function $\Psi(\mathbf{r})$, which is often easier to obtain. This is evident by the fact that ρ depends only on three spatial coordinates, whereas Ψ depends on $3N$ spatial coordinates where N is the number of electrons in the system.

Thanks to the work of W. Kohn and L. J. Sham (KS) in 1965 [3], DFT was set and ready to provide a practical framework to employ the electronic density as the primary variable, as first envisioned by L. Thomas, E. Fermi and P. Dirac [5, Ch. 3]. Replacing the wave-function of a many-body quantum system by the density not only made the problem simpler to work with analytically, but also made it more computationally efficient to achieve a higher level of accuracy. KS provided a framework in which the HK theorems become applicable; they introduced a fictitious system of non-interacting fermions where the exact wave-function for said system is a Slater determinant Φ_{KS} with orbitals $\{\theta_i\}_{i=1}^N$ in analogy to HF. Furthermore, they divided the universal functional $F[\rho(\mathbf{r})]$ into three parts as follows:

$$F[\rho] = T_0[\rho] + J[\rho] + E_{xc}[\rho] \tag{1.11}$$

where $T_0[\rho]$ is the kinetic energy of the non-interacting system, $J[\rho] = \frac{1}{2}\int\int \rho(\mathbf{r}_1)\rho(\mathbf{r}_2)d\mathbf{r}_1 d\mathbf{r}_2$ is the classical Coulomb repulsion, $E_{xc}[\rho] = T_{xc}[\rho] + J_{xc}[\rho]$ is the so called *exchange-correlation* energy functional which contains kinetic and interaction energy parts due to the real system consisting of interacting fermions. E_{xc} can be thought of as the complicated portion of the energy of the system. KS also required that the non-interacting system must have the same density as the GS density of the system under study, that is:

$$\rho_{\text{KS}}(\mathbf{r}) = \sum_s \sum_{i=1}^N |\theta_i(\mathbf{r}, s)|^2 = \rho_0(\mathbf{r}) \tag{1.12}$$

where N here denotes the number of occupied orbitals and $s \in \{\uparrow, \downarrow\}$. To abide by the restriction on the density profile in (1.12), one must solve the KS equations given by:

$$\left[-\frac{1}{2}\nabla^2 + V_{\text{KS}}(\mathbf{r})\right]\theta_i = \mu_i\theta_i \tag{1.13}$$

where V_{KS} is defined as:

$$V_{\text{KS}}(\mathbf{r}) \equiv V_{\text{ext}}(\mathbf{r}) + V_J(\mathbf{r}) + V_{xc}(\mathbf{r}) = V_{\text{ext}}(\mathbf{r}) + \frac{\delta J[\rho]}{\delta\rho(\mathbf{r})} + \frac{\delta E_{xc}[\rho]}{\delta\rho(\mathbf{r})}. \tag{1.14}$$

Since V_{KS} depends on the density ρ, the KS equations given by (1.13) must be solved self-consistently analogous to the HF equations which we shall introduce in the next chapter. Once self-consistency has been reached in the solution, the ground state density $\rho_0(\mathbf{r})$ can be calculated using (1.12) followed by all properties such as E_0. However, things practically are not as sound as on paper; the possibility of representing an arbitrary ground state density by a system of non-interacting fermions hinges on the existence of V_{xc}; otherwise, the problem can not be solved using this scheme [20]. This is due to the fact that V_{ext} and V_J are relatively easy to calculate. V_J is explicitly known and V_{ext} depends on the system, so this leaves the kinetic energy part of the non-interacting system and V_{xc} (which is the most problematic).

While exact in principle, to be made practical DFT requires the use of approximations. The most

notorious quantity in a DFT calculation, as mentioned above, is the exchange-correlation potential V_{xc} which is non-local in principle. The non-locality of V_{xc} makes an exact calculation rather tedious and unachievable in cases of large systems, analogous to E_x in the HF scheme. The main problem is therefore to find a suitable approximation for the exchange-correlation potential that is computationally applicable, whilst quantitative results regarding the system under study remain accessible. Such approximation can be obtained by extracting the exchange-correlation potential from an infinite reference system where V_{xc}^{ref} is not necessarily non-local, i.e. $V_{xc}^{\text{ref}}[\rho] = V_{xc}^{\text{ref}}(\rho)$. An example is that of LDA where the reference system used is the homogenous electron gas (Jellium) which is solvable in an exact numerical manner [25]. The LDA for V_{xc} is given by:

$$V_{xc}^{\text{LDA}} = \frac{\delta E_{xc}^{\text{LDA}}}{\delta \rho(\mathbf{r})} = \epsilon_{xc}(\rho(\mathbf{r})) + \rho(\mathbf{r}) \frac{\delta \epsilon_{xc}(\rho)}{\delta \rho} \tag{1.15}$$

where $\epsilon_{xc}(\rho)$ is the exchange-correlation energy per particle of a uniform electron gas of density ρ [4].

It has been shown by K. Schönhammer, O. Gunnarsson and R. M. Noack in 1995 that the concept of DFT applies not only to functionals of the density ρ in the continuous case, but to any functional of a function that is *non-interacting v-representable* in what they called "$\{A\}$*-functional theory*" [6]. This is for example the case of the Hubbard model, which describes lattice systems where electrons can hop to neighboring sites (tight-binding part) and interact with other electrons localized at the same site (local interaction part) [2]. One generalized-DFT-like theory for lattice systems is *site-occupation-functional theory* (SOFT) where the site occupation number[2] $\langle \hat{n} \rangle$ (which we call density) assumes the role of the density $\rho(\mathbf{r})$ in the continuous case[3] [7]. In one dimension, the reference system for LDA, i.e. the one-dimensional homogenous Hubbard model, is exactly solvable. The solution uses the Bethe-ansatz and the details are not relevant for our work [8]. However, this made it possible to construct an exact LDA for the discrete case, i.e. the Bethe-ansatz local density approximation (BALDA) for one-dimensional lattice systems. V_{xc} is approximated using[4]:

$$\begin{aligned} V_{xc}^{\text{BALDA}}(\langle \hat{n} \rangle < 1) &= -2\cos\left(\frac{\pi \langle \hat{n} \rangle}{\beta(U)}\right) + 2\cos\left(\frac{\pi \langle \hat{n} \rangle}{2}\right) - \frac{U \langle \hat{n} \rangle}{2} \\ V_{xc}^{\text{BALDA}}(\langle \hat{n} \rangle > 1) &= +2\cos\left(\frac{\pi (2 - \langle \hat{n} \rangle)}{\beta(U)}\right) - 2\cos\left(\frac{\pi (2 - \langle \hat{n} \rangle)}{2}\right) + \frac{U(2 - \langle \hat{n} \rangle)}{2} \end{aligned} \tag{1.16}$$

where U is the local interaction strength (see section 2.2) and $\beta(U)$ is given by the solution to the transcendental equation:

$$\frac{\beta(U)}{\pi} \sin\left(\frac{\pi}{\beta(U)}\right) = 2 \int_0^\infty \frac{J_0(x) J_1(x)}{x \left(1 + e^{Ux/2}\right)} dx, \tag{1.17}$$

[2] Defined as the expectation value of the number operator $\hat{n}$ to be defined in the next chapter.

[3] See also the work by Gunnarsson and Schönhammer [21].

[4] Strictly speaking, the approximation given by (1.16) is not exact since Capelle's interpolation is an approximation itself, however, it is believed to be a good one (see [9] or [10]).

where $J_0(x)$ and $J_1(x)$ are Bessel functions of the first kind [10]. The graph of V_{xc}^{BALDA} at different values of the parameter U is shown in Figure 1.1. The discontinuity around half-filling $\langle \hat{n} \rangle = 1$ is a characteristic of V_{xc} when $U > 0$ that manifests the Mott metal-insulator transition for the one-dimensional Hubbard model [9].

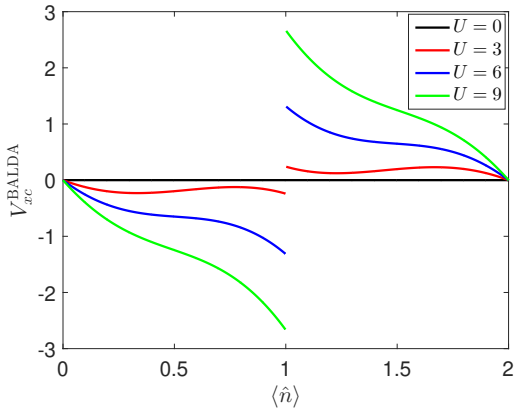

Figure 1.1: V_{xc}^{BALDA} as a function of the density $\langle \hat{n} \rangle$ according to (1.16) and (1.17) at different values of U. Note the discontinuity at $\langle \hat{n} \rangle = 1$. This figure is a reproduction of [10, Fig. 2].

We end this section by presenting results of applying BALDA to $N = 14$ electrons in the spin compensated case ($N_\uparrow = N_\downarrow = 7$) on a one-dimensional lattice of $L = 21$ sites trapped in a parabolic potential on the form:

$$V_p(i) = p(i - \lceil L/2 \rceil)^2 \tag{1.18}$$

where i denotes the site index and p is a real number. A comparison between the density profiles obtained in the cases of employing BALDA and without V_{xc} for $p = 0.5$ and two different values of U is shown in Figure 1.2. The hopping parameter t (see section 2.2) is set to 1 in all cases presented in this thesis. Note that the correction to the density profile offered by BALDA is pronounced when the interaction strength U dominates over the effect of the external potential p. It is also clear in the $U = 6$ case the effect of the discontinuity in V_{xc}^{BALDA} around half-filling on the density profile.

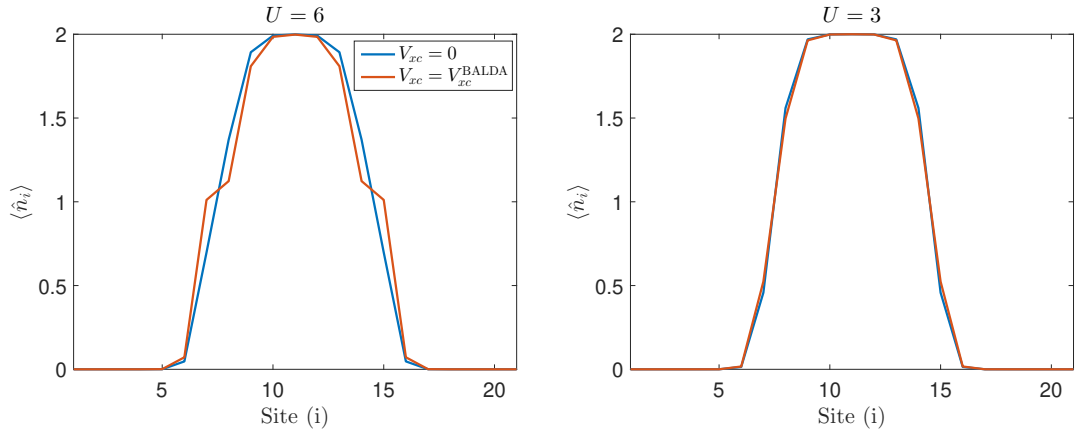

Figure 1.2: A figure that shows a comparison between employing BALDA for V_{xc} and the case of neglecting exchange-correlation effects all together. The density $\langle \hat{n}_i \rangle$ is plotted as a function of the site index i for two different systems. The left panel shows $U = 6$ while the right panel shows $U = 3$.

1.3 Scope of this work

The work presented by this thesis, as mentioned previously, aims to compare an approximation for long-ranged electronic interaction that is not entirely local to a local approximation for the same interaction. Ideally, said interactions would be the exchange and correlation and an approximation would be formulated in the spirit of BALDA. Furthermore, BALDA would be the local approximation to compare with. However, BALDA is built from a reference system that is analytically solvable, i.e. the homogenous Hubbard model [8]. To expand such approximation to include non-local effects, say nearest neighbors, we would like to get an expression on the form:

$$V_{xc}[\langle \hat{n}_i \rangle] \approx V_{xc}^{\text{ref}} = V_{xc}^{\text{ref}}(\langle \hat{n}_{i-1} \rangle, \langle \hat{n}_i \rangle, \langle \hat{n}_{i+1} \rangle), \tag{1.19}$$

where $\langle \hat{n}_{i-1} \rangle$, $\langle \hat{n}_i \rangle$ and $\langle \hat{n}_{i+1} \rangle$ can be different. However, no analytical solution is known for the reference system we would want to extract V_{xc}^{ref} from; a not-entirely-homogenous Hubbard model. Albeit it is not possible to construct an approximation in the same way as BALDA, this approach can still be tested at another level to gain an intuition and set the stage for a more thorough treatment. We will refrain from discussing V_{xc} any further in this thesis and we will focus on a simpler approach to the problem that is analytically solvable, i.e. the HF approximation for the extended Hubbard model. In this context, HF will act as an exact solution and the long-ranged interaction potential in the extended Hubbard model will be the approximated potential. We will also offer a characterization of the HF solution in the case of local interaction only and how to extend this work in the future. The work presented will only address the case of one dimension and the case of higher dimensions is left to future work. We only considered local interaction in characterizing the HF solution via numerical results due to lack of time to include long-ranged interaction as the problem is non-trivial. The restriction to the HF approximation is also a result of the limited time assigned to the project.

Chapter 2

Theory

2.1 The Hartree-Fock approximation: A closer look

Given that we set HF to be our focus, this section is aimed towards presenting some details of the theory as well as fill any gaps left by the Introduction. The following part is based on [4, Sec. 1.3] and [5, Sec. 1.3]. Let us now look at the HF solution for a many-body system described by the Hamiltonian given by equation (1.7). Furthermore, suppose that the operator $\hat{V}_{\text{ext}}$ has a spatial representation which can be written as:

$$\hat{V}_{\text{ext}} = \sum_{i=1}^{N} v(\mathbf{r}_i) \tag{2.1}$$

where $v(\mathbf{r}_i)$ is the external potential felt by the i^{th} electron (for example, $\hat{V}_{\text{ext}}$ can be the operator of the total energy of the interaction between the electrons of the system and stationary nuclei in the Born-Oppenheimer limit). The HF energy (equation (1.4)) is then given by:

$$E_{\text{HF}} = \underbrace{\sum_{i}^{N} h_i}_{E_{\text{k}}+E_{\text{ext}}} + \underbrace{\frac{1}{2}\sum_{ij}^{N}(J_{ij} - K_{ij})}_{E_{ee}} \tag{2.2}$$

where E_{k} is the kinetic energy, E_{ext} is the energy due to the external potential and E_{ee} is the electron-electron interaction energy. h_i, J_{ij} and K_{ij} are given by[1]:

$$\begin{aligned} h_i &= \int \aleph_i^*(\mathbf{x})(-\frac{1}{2}\nabla^2 + v(\mathbf{r}))\aleph_i(\mathbf{x})d\mathbf{x} \\ J_{ij} &= \int\int \aleph_i(\mathbf{x}_1)\aleph_i^*(\mathbf{x}_1)\frac{1}{|\mathbf{r}_1 - \mathbf{r}_2|}\aleph_j^*(\mathbf{x}_2)\aleph_j(\mathbf{x}_2)d\mathbf{x}_1 d\mathbf{x}_2 \\ K_{ij} &= \int\int \aleph_i^*(\mathbf{x}_1)\aleph_j(\mathbf{x}_1)\frac{1}{|\mathbf{r}_1 - \mathbf{r}_2|}\aleph_i(\mathbf{x}_2)\aleph_j^*(\mathbf{x}_2)d\mathbf{x}_1 d\mathbf{x}_2 \end{aligned} \tag{2.3}$$

and the orbitals $\{\aleph_i(\mathbf{x})\}_{i=1}^{N}$ are defined as in (1.2). J_{ij} and K_{ij} are called the Coulomb and exchange integrals respectively. In order to find the set of orbitals $\{\aleph_i(\mathbf{x})\}_{i=1}^{N}$ that minimizes the energy according to equation (1.3), one must solve the HF equations (analogous to the KS equations (1.13)) given by[2]:

$$\begin{aligned} \hat{f}\aleph_i(\mathbf{x}) &= \epsilon_i\aleph_i(\mathbf{x}) \\ \hat{f} &= -\frac{1}{2}\nabla^2 + v(\mathbf{r}) + V_{\text{HF}}(\mathbf{x}) \end{aligned} \tag{2.4}$$

[1] For notation, see Appendix A.

[2] Under the constraint that the orbitals $\{\aleph_i(\mathbf{x})\}_{i=1}^{N}$ are normalized.

where the eigenvalues $\{\epsilon_i\}_{i=1}^N$ are the orbital energies, $\hat{f}$ is the Fock operator and V_{HF} is the HF potential which reads:

$$\hat{V}_{\text{HF}} = \sum_{i=1}^{N} \hat{j}_i - \hat{k}_i, \tag{2.5}$$

here $\hat{j}$ and $\hat{k}$ are the Coulomb and exchange operators respectively, given by:

$$j_i(\mathbf{x}_1) = \int \left|\aleph_i(\mathbf{x}_2)\right|^2 \frac{1}{r_{12}} d\mathbf{x}_2 \tag{2.6}$$

$$k_i(\mathbf{x}_1)\aleph_j(\mathbf{x}_1) = \aleph_i(\mathbf{x}_1) \int \aleph_i^*(\mathbf{x}_2) \frac{1}{|\mathbf{r}_1 - \mathbf{r}_2|} \aleph_j(\mathbf{x}_2) d\mathbf{x}_2. \tag{2.7}$$

Needless to say, the HF potential depends on the orbitals $\{\aleph_i(\mathbf{x})\}_{i=1}^N$ and (2.4) should be solved self-consistently (analogous to the KS equations (1.13)) which is what granted the method the name: *The self-consistent field*. We will encounter a correspondence in the self-consistency requirement when we turn to a DFT (or rather SOFT) treatment of HF in the next section. However, the solution then would depend on the *density* and not the *orbitals* which are equivalent when discussing the GS.

We end this section with some remarks to link it to what we presented in the first part of the Introduction. The HF potential $V_{\text{HF}}(\mathbf{x})$ when acting on the spin orbital $\aleph_i$ represents the average Coulomb repulsion ($\hat{j}$ part) felt by the i^{th} electron due to the remaining electrons, and in addition a non-local exchange contribution ($\hat{k}$ part) imposed by the anti-symmetry of the total wave-function. Accounting for the classical Coulomb repulsion only in average is what gave rise to equation (1.6). What is meant by the non-locality of the exchange part in $V_{\text{HF}}(\mathbf{x})$ can be readily seen in equation (2.7). Note that when the operator $\hat{k}_i$ acts on the orbital $\aleph_j(\mathbf{x}_1)$, the result does not depend only on the value of $\aleph_j$ at $\mathbf{x}_1$, but on all points in space in contrary to the operator $\hat{j}_i$, which is local. Furthermore, the expectation values of $\hat{j}_i$ and $\hat{k}_i$ are nothing but the Coulomb and exchange integrals given by (2.3) and the non-locality in E_x ($-1/2\sum_{i\neq j} K_{ij}$) follows[3]. Finally, the results presented in this thesis are for an even number of electrons in the spin-compensated case, i.e. the *restricted HF* (RHF). However, we will not discuss more than the general attributes of the HF method in the continuous case presented in this section. In the next section, we will consider the HF approximation for a one-dimensional lattice system and change our basic variable from being an orbital to an occupation number.

2.2 Density-functionalising Hartree-Fock: The Hartree-Fock approximation for the extended Hubbard model

This section is aimed at looking at the Hubbard model under the HF approximation. In this regime, our system will be a one-dimensional lattice and our basic variable will be the site-occupation

[3]Here we use $i \neq j$ to avoid the non-physical self-interaction term which is canceled in the full expression by virtue of $J_{ii} = K_{ii}$.

number $\langle \hat{n}_i \rangle$ (i is the site index) as appropriate for DFT calculations performed on a lattice, i.e. SOFT [7]. The Hubbard Hamiltonian, first introduced by John Hubbard in 1963, is a lattice model used to describe localized electrons around stationary nuclei (under the Born-Oppenheimer approximation) where a lattice description is appropriate [2]. The electrons interact only with other electrons localized at the same nucleus (site) and the model was successfully employed to describe electron correlations in narrow energy bands [13]. The one-dimensional Hubbard Hamiltonian $\hat{H}_0$ in its simplest form in second quantization formalism is given by:

$$\hat{H}_0 = -\sum_{\langle i,j \rangle \sigma} t_{ij} \hat{c}^\dagger_{i\sigma} \hat{c}_{j\sigma} + U \sum_i \hat{n}_{i\uparrow} \hat{n}_{i\downarrow} \tag{2.8}$$

where the notation $\langle i, j \rangle$ denotes ordered pairs of nearest neighbors, $\sigma \in \{\uparrow, \downarrow\}$, t_{ij} are the hopping matrix elements, $\hat{c}^\dagger_{i\sigma}$ and $\hat{c}_{j\sigma}$ denote creation and annihilation operators of an electron with spin σ at sites i and j respectively, U is the on-site interaction strength and $\hat{n}_{i\uparrow} = \hat{c}^\dagger_{i\uparrow} \hat{c}_{i\uparrow}$ and $\hat{n}_{i\downarrow} = \hat{c}^\dagger_{i\downarrow} \hat{c}_{i\downarrow}$ are number operators. t and U set the energy scale and determine the relative strength of the two sums that contribute to the Hamiltonian. In this thesis it will be assumed that the hopping matrix elements are given by $t_{ij} = t$ between nearest neighbors and $t_{ij} = 0$ otherwise.

For arbitrary sites i and j, consider the following representation of the spin dependent density operators $\hat{n}_{i\sigma}$ and $\hat{n}_{j\beta}$ where $\sigma, \beta \in \{\uparrow, \downarrow\}$:

$$\begin{aligned} \hat{n}_{i\sigma} &= \langle \hat{n}_{i\sigma} \rangle + \hat{n}_{i\sigma} - \langle \hat{n}_{i\sigma} \rangle = \langle \hat{n}_{i\sigma} \rangle + \delta \hat{n}_{i\sigma} \\ \hat{n}_{j\beta} &= \langle \hat{n}_{j\beta} \rangle + \hat{n}_{j\beta} - \langle \hat{n}_{j\beta} \rangle = \langle \hat{n}_{j\beta} \rangle + \delta \hat{n}_{j\beta}. \end{aligned} \tag{2.9}$$

Multiplying $\hat{n}_{i\sigma}$ and $\hat{n}_{j\beta}$, we find:

$$\hat{n}_{i\sigma} \hat{n}_{j\beta} = \langle \hat{n}_{i\sigma} \rangle \hat{n}_{j\beta} + \langle \hat{n}_{j\beta} \rangle \hat{n}_{i\sigma} - \langle \hat{n}_{i\sigma} \rangle \langle \hat{n}_{j\beta} \rangle + \delta \hat{n}_{i\sigma} \delta \hat{n}_{j\beta}. \tag{2.10}$$

By setting the product of fluctuations $\delta \hat{n}_{i\sigma} \delta \hat{n}_{j\beta}$ to zero, we apply a mean-field approximation to equation (2.10). Furthermore, the quantity $\langle \hat{n}_{i\sigma} \rangle \langle \hat{n}_{j\beta} \rangle$ will only contribute to the total energy of the system which has no relevance to our calculations and can be safely neglected. Under said assumptions, equation (2.10) reads:

$$\hat{n}_{i\sigma} \hat{n}_{j\beta} \approx \langle \hat{n}_{i\sigma} \rangle \hat{n}_{j\beta} + \langle \hat{n}_{j\beta} \rangle \hat{n}_{i\sigma}. \tag{2.11}$$

If we now combine equations (2.8) and (2.11) we get the Hamiltonian:

$$\hat{H}_0^{\text{HF}} = -t \sum_{\langle i,j \rangle \sigma} \hat{c}^\dagger_{i\sigma} \hat{c}_{j\sigma} + U \sum_{i\sigma} \langle \hat{n}_{i,-\sigma} \rangle \hat{n}_{i\sigma}. \tag{2.12}$$

The above equation is what some people call the Hubbard Hamiltonian under the Hartree-Fock approximation (for example John Hubbard) [2]. However, some people will reserve the name Hartree-Fock for a mean-field treatment that preserves the spin rotational invariance of the origi-

nal Hubbard model given by (2.8), which would explicitly contain a spin dependent term for the exchange part (for example Frank Lechermann) [12, Ch. 3]. Therefore, the above treatment neglects the Fock part and the resulting Hamiltonian only contains the Hartree approximation, or simply, a mean-field. To avoid ambiguity, such treatment will always have the name Hartree-Fock in this thesis since it preserves the property of having a linear potential for electronic interaction analogous to RHF.

In order to be able to test different approximations for electronic interactions, we need to include a long-ranged interaction term in the Hamiltonian. This can be applied by adding a non-local term to the original Hubbard Hamiltonian. The extended Hubbard Hamiltonian $\hat{H}_1$ then reads:

$$\hat{H}_1 = \hat{H}_0 + \frac{1}{2}\sum_{i\neq j} U_{ij}\hat{n}_i\hat{n}_j \tag{2.13}$$

where U_{ij} denotes the interaction strength between the sites i and j, $\hat{n}_i = \hat{n}_{i\uparrow} + \hat{n}_{i\downarrow}$ and $\hat{n}_j = \hat{n}_{j\uparrow} + \hat{n}_{j\downarrow}$. Note that, unlike the local interaction term, interaction between electrons of the same spin is permitted (in the local case it would be a non-physical self-interaction).

One can easily find by combining equation (2.13) and the approximation (2.11), and using the fact that $U_{ij} = U_{ji}$ that the HF approximation for $\hat{H}_1$ is given by:

$$\hat{H}_1^{\text{HF}} = \hat{H}_0^{\text{HF}} + \sum_{i\neq j} U_{ij}\langle\hat{n}_j\rangle\hat{n}_i. \tag{2.14}$$

If the system under study is subject to an external potential or an additional perturbation, we add it to the Hamiltonian $\hat{H}_1$ via:

$$\begin{aligned}\hat{H}^{\text{HF}} &= \hat{H}_1^{\text{HF}} + \sum_i v_i\hat{n}_i \\ &= -t\sum_{\langle i,j\rangle\sigma}\hat{c}^\dagger_{i\sigma}\hat{c}_{j\sigma} + U\sum_{i\sigma}\langle\hat{n}_{i,-\sigma}\rangle\hat{n}_{i\sigma} + \sum_{ij}U_{ij}(1-\delta_{ij})\langle\hat{n}_j\rangle\hat{n}_i + \sum_i v_i\hat{n}_i\end{aligned} \tag{2.15}$$

where v_i denotes the additional potential. In general, an additional perturbation might be spin dependent. However, we restrict the focus to spin independent modifications in the present work. Equation (2.15) is the general form of the HF Hamiltonian we will work with in this thesis. Note that if one wishes to diagonalize $\hat{H}_{\text{HF}}$, the solution should be self-consistent since the interaction terms in (2.15) depend explicitly on the density profile, which is what we called *"the self-consistency correspondence"* in the previous section. In the next section, we will show how to obtain a local approximation for the long-ranged interaction term in $\hat{H}^{\text{HF}}$.

2.3 Long-ranged interaction: A local approximation within Hartree-Fock

In analogy to BALDA, where the reference system is the one-dimensional homogenous Hubbard model which is, as mentioned in the Introduction, analytically solvable using the Bethe-ansatz [8], we aim to find a *local (density) approximation* (for which we will use the acronym LHFA to avoid confusion with the acronym LDA) that fits into the Hartree-Fock picture. BALDA provides us with an LDA to the exchange-correlation potential extracted from an infinite model of the system under study where all sites have the same density [10]. In our case, we want to find an LHFA to the potential given by:

$$V_i = \sum_j U_{ij}(1-\delta_{ij})\langle \hat{n}_j \rangle. \tag{2.16}$$

Assuming a corresponding infinite homogenous reference system (Figure 2.1 up) where $\langle \hat{n}_j \rangle = \langle \hat{n}_i \rangle = \langle \hat{n}^{\text{ref}} \rangle$ for all i and j and $U_{ij} = U(|i-j|)$, we get:

$$V_i^{\text{LHFA}} = \langle \hat{n}_i \rangle \sum_j U(|i-j|)(1-\delta_{ij}). \tag{2.17}$$

Since the system is infinite, the site i will have an infinite number of sites to the left and right of it, thus the summation in the above equation can be written as:

$$\begin{aligned} \sum_j U(|i-j|)(1-\delta_{ij}) &= \underbrace{(U(1)+U(2)+U(3)+...)}_{\text{left of } i} + \underbrace{(U(1)+U(2)+U(3)+...)}_{\text{right of } i} \\ &= 2(U(1)+U(2)+U(3)+...) = 2\sum_{k=1}^{\infty} U_k \end{aligned} \tag{2.18}$$

where $U_k = U(k) = U(|i-j|=k)$. Finally, by combining equations (2.18) and (2.17), we arrive at the following result:

A 1. *The local approximation $V_i^{LHFA} = V^{LHFA}(\langle \hat{n}_i \rangle)$ for the long-ranged interaction potential* (2.16) *is given by:*

$$V_i^{LHFA} = 2\langle \hat{n}_i \rangle \sum_{k=1}^{\infty} U_k, \tag{2.19}$$

here **A 1** denotes **Approximation 1**. In the next section, we will present a near-local approximation (NLA) for V_i based on a system that is not entirely homogenous.

2.4 Long-ranged interaction: A near-local approximation within Hartree-Fock

If we want to find an approximation for V_i based on a reference system that is not entirely homogenous, the task gets more complicated than that of the previous section. In this thesis, the reference system we used has a degree of homogeneity up to three consecutive sites. That is, the

system can be divided into unit cells where each unit cell contains three different sites. Each site is identical to its counterpart in other unit cells. A comparison between said reference system and the homogenous reference system used in the previous section is shown in Figure 2.1.

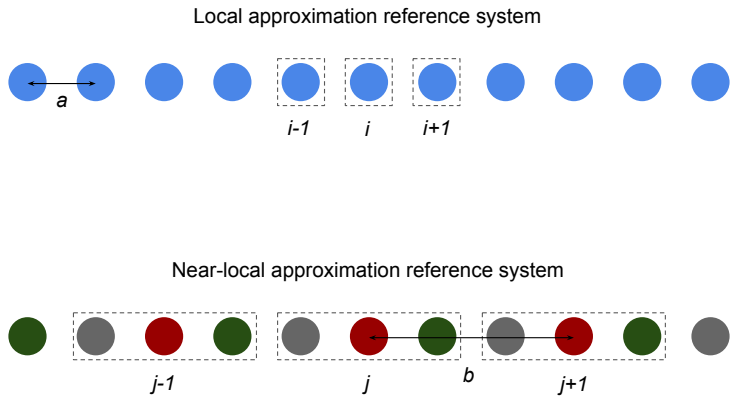

Figure 2.1: A sketch that shows a comparison between the homogenous reference system used in the previous section for LHFA and the reference system we aim to use in the NLA case. The number of sites chosen in the sketch is only intended to show the general characteristics of each system. The unit cell index for the homogenous model is i and the lattice constant is a, while for the reference system used in this section, the unit cell index is j and the lattice constant is b.

It is rather natural to introduce the degree of freedom $\alpha \in \{l, c, r\}$ where l denotes *left*, c denotes *center* and r denotes *right*. For the reference system in question, each unit cell will contain three sites with corresponding densities $\langle \hat{n}_l \rangle$, $\langle \hat{n}_c \rangle$ and $\langle \hat{n}_r \rangle$ from left to right. This is true for all unit cells since the system has a degree of homogeneity up to three consecutive sites. In this notation, the long-ranged interaction part of the Hamiltonian $\hat{H}_{\text{LR}} = \sum_{i \neq j} U_{ij} \langle \hat{n}_j \rangle \hat{n}_i$ as in (2.15) reads:

$$\hat{H}_{\text{LR}}^{\text{NLA}} = \sum_{j\alpha j'\alpha'} U_{j\alpha j'\alpha'} (1 - \delta_{jj'}\delta_{\alpha\alpha'}) \langle \hat{n}_{j'\alpha'} \rangle \hat{n}_{j\alpha} \tag{2.20}$$

where the subscript LR denotes the long-ranged interaction part of the Hamiltonian, j and j' here denote unit cell indices and α and α' denote the *left*, *center* or *right* sites within the unit cells with indices j and j' respectively. The above equation does not add or take anything from the expression given by equation (2.15) for $\hat{H}_{\text{LR}}$, rather, it is merely a reformulation for our reference system. From equation (2.20) we can immediately see that the potential V_i^{NLA} (now $V_{j\alpha}^{\text{NLA}}$) is given by:

$$V_{j\alpha}^{\text{NLA}} = \sum_{j'\alpha'} U_{j\alpha j'\alpha'} (1 - \delta_{jj'}\delta_{\alpha\alpha'}) \langle \hat{n}_{j'\alpha'} \rangle. \tag{2.21}$$

The above expression suggests 3 different possible values for V_i^{NLA}. This is the starting point to arrive at the final expression for V_i^{NLA}. We end this section by presenting the approximation A 2 which offers us three variants (one for each value of α) of the near-local approximation, namely the *left* site approximation (LSA), the *center* site approximation (CSA) and the *right* site approximation (RSA). The details behind arriving at A 2 are given in Appendix B.

A 2. *The near-local approximation* $V_i^{NLA} = V^{NLA}(\langle \hat{n}_{cell} \rangle)$ *for the long-ranged interaction potential* (2.16) *can be obtained in three distinct ways given by:*

$$V_i^{NLA} = \langle \hat{n}_{cell} \rangle \sum_{k=1}^{\infty} U_k (1 - \delta_{0mod(k,3)}) + \langle \hat{n}_i \rangle \sum_{k=1}^{\infty} (3U_{3k} - U_k)$$

$$\langle \hat{n}_{cell} \rangle = \begin{cases} \langle \hat{n}_i \rangle + \langle \hat{n}_{i+1} \rangle + \langle \hat{n}_{i+2} \rangle & LSA \\ \langle \hat{n}_i \rangle + \langle \hat{n}_{i+1} \rangle + \langle \hat{n}_{i-1} \rangle & CSA \\ \langle \hat{n}_i \rangle + \langle \hat{n}_{i-1} \rangle + \langle \hat{n}_{i-2} \rangle & RSA \end{cases} . \tag{2.22}$$

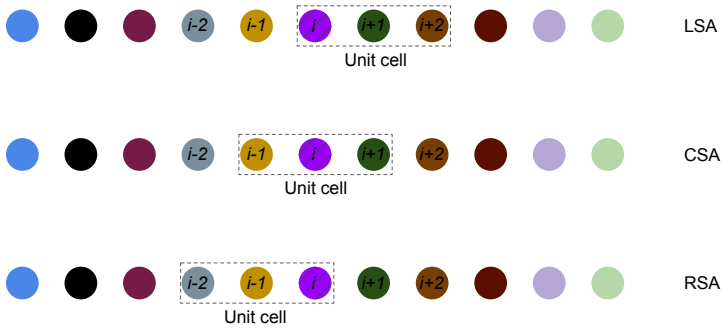

Figure 2.2: A sketch that shows the different ways to approximate the long-ranged interaction potential at site i of any inhomogeneous system under consideration according to NLA. Each approximation defines a different unit cell, hence, a different reference system.

This non-uniqueness in the approximation presented by NLA is the price we pay for the α degree of freedom as explained in the derivation. The two equations given by (2.22) offer three different ways to approximate V_i from a reference system that is homogenous up to three consecutive sites, namely, LSA, CSA and RSA. To construct the total density of one unit cell, LSA considers the value of the density at a given reference site i and the density at a pair of sites succeeding i, CSA considers the density at i and the density of the two sites nearest to i and RSA considers the density at i and the density at a pair of sites preceding i. If an answer to the question: which one is the best approximation? did exist, it is definitely not intuitive. There is no clear reason why one would perform better than the other, however, they are definitely different approximations in general. This leaves the preferred protocol to be determined via assessment over different systems under study. We need to emphasize however, that the approximations LSA, CSA and RSA only differ from each other in the choice of $\langle \hat{n}_{\text{cell}} \rangle$. Formally, this choice is arbitrary since *left*, *center* and *right* are a matter of convention. Therefore, in principle the approximations are not different, rather, our choice of the unit cell is the only factor that determines the value of the potential. Regardless of which value of $\langle \hat{n}_{\text{cell}} \rangle$ is used to calculate V_i^{NLA}, we can make a comparison between the local approximation and an approximation that takes into account neighboring sites using all variants given by (2.22). However, to make an accurate statement, we need to take all of them into account.

2.5 A characterization of the Hartree-Fock solution via the density of states

In this section, we will provide a characterization of the HF solution for the reference system discussed in the previous section in the case of local interaction only (U). We will consider the spinless case only in this section since extending our discussion to include spin in the RHF scheme (spin-compensated case) would only require a multiplication by 2. That is, from (2.15), we will be looking at the Hamiltonian given by:

$$\hat{H}_{\text{HF}}^{\text{ref}} = \underbrace{-t \sum_{\langle j\alpha, j'\alpha' \rangle} \hat{c}_{j\alpha}^{\dagger} \hat{c}_{j'\alpha'}}_{\hat{H}_{\text{TB}}^{\text{ref}}} + \underbrace{\sum_{j\alpha} \epsilon_{\alpha} \hat{n}_{j\alpha}}_{\hat{H}_{\epsilon}^{\text{ref}}} + \underbrace{U \sum_{j\alpha} \langle \hat{n}_{j\alpha} \rangle \hat{n}_{j\alpha}}_{\hat{H}_{U}^{\text{ref}}} \tag{2.23}$$

where we dispose of the spin degree of freedom by omitting the summation over σ and adapt the notation from the previous section otherwise. Note the term $\hat{H}_{\epsilon}^{\text{ref}}$ which gives rise to the α degree of freedom, here $\{\epsilon_{\alpha}\}_{\alpha}$ are real numbers which represent the different energy shifts within one unit cell. The main attributes of $\hat{H}_{\text{HF}}^{\text{ref}}$ will be given on the form of analytical expressions[4], namely, the energy dispersion with respect to the wave-vector which we call k and the density of states (DoS) f.

First, let us look at an example to make clear what we mean by the energy dispersion. Consider the spinless tight-binding Hamiltonian given by:

$$\hat{H}_{\text{TB}} = -t \sum_{\langle i,j \rangle} \hat{c}_i^{\dagger} \hat{c}_j \tag{2.24}$$

where i and j here are site indices. For a system described by $\hat{H}_{\text{TB}}$, with lattice constant $a = 1$ and under periodic boundary conditions[5], the following relation holds:

$$E_k = -2t \cos k \tag{2.25}$$

where $k = (2\pi/\lambda) \in [-\pi, \pi)$ is the wave-vector in the first Brillouin zone and λ is the wavelength. Equation (2.25) is called the energy dispersion formula for $\hat{H}_{\text{TB}}$ and coincides with [11, Exercise 1.3]. A derivation is provided in Appendix B since it is analogous to that of the next statement, which provides us with the energy dispersion formula for our last reference system.

Statement 1. *For a system described by the Hamiltonian* (2.23)*, under periodic boundary conditions and with the lattice constant $b = 1$, the allowed energy values for a given wave-vector k in the first Brillouin zone are given by:*

$$\{E_{km}\}_{m=1}^{3} = \text{eig}(\boldsymbol{A}_k) \tag{2.26}$$

[4]The derivations are given as appendices for the sake of readability.
[5]Born-von Karman, 1912.

where $\boldsymbol{A}_k$ is 3x3 and reads:

$$\begin{aligned} \boldsymbol{A}_k &= \begin{pmatrix} D_c & -t & -t \\ -t & D_l & -te^{-ik} \\ -t & -te^{ik} & D_r \end{pmatrix} \\ D_c &= \epsilon_c + U\langle \hat{n}_c \rangle \\ D_l &= \epsilon_l + U\langle \hat{n}_l \rangle \\ D_r &= \epsilon_r + U\langle \hat{n}_r \rangle \end{aligned} \tag{2.27}$$

where D_l, D_c and D_r are different energy shifts at the *left*, *center* and *right* sites of any given unit cell in the system. A derivation of Statement 1 can be found in Appendix B. Statement 1 gives rise to an immediate result, namely the following:

Statement 2. *The energy eigenstates for the Hamiltonian given in* (2.23) *are the eigenvectors of* $\{\boldsymbol{A}_{k_p}\}_p$ *denoted by* $\{|k_p m\rangle\}_{pm}$ *where* $m \in \{1, 2, 3\}$. *Furthermore, given an arbitrary, yet allowed,* $k_p = k$ *in the first Brillouin zone, the energy eigenstates* $\{|km\rangle\}_m$ *corresponding to the energies* $\{E_{km}\}_m$ *as given in Statement 1, are given by:*

$$|km\rangle = \sum_{\alpha} C_{\alpha}^{km} |k\alpha\rangle, \quad \alpha \in \{c, l, r\} \tag{2.28}$$

where C_c^{km}, C_l^{km} and C_r^{km} denote the first, second and third entry of the 3-dimensional vector $|km\rangle$, respectively. The importance of the above statements will become more clear after combining them with the following result; they will provide us with means to calculate the density of states, and hence, the density profile for the system.

Statement 3. *For the system described by the Hamiltonian given in* (2.23) *in the ground state, the center, left, and right densities* $\{\langle \hat{n}_\alpha \rangle\}_\alpha$ *within one unit cell are given by:*

$$\langle \hat{n}_\alpha \rangle = \int_{-\infty}^{\mu} f_\alpha(E) dE = \frac{1}{L} \int_{-\infty}^{\mu} \sum_{pm} \left| C_\alpha^{k_p m} \right|^2 \delta\left(E - E_{k_p m}\right) dE \tag{2.29}$$

where $f_\alpha(E)$ is the density of states at site α normalized to 1, μ is the chemical potential and the coefficients $\{C_\alpha^{k_p m}\}_{pm}$ and the energy values $\{E_{k_p m}\}_{pm}$, are given in accordance with Statement 2 and Statement 1, respectively. A derivation of Statement 3 is given in Appendix B.

The above results allow us to study the reference system for NLA from a different perspective. Although only local interactions were taken into account, qualitative results can still be obtained for the DoS. The solution would be a characteristic of the reference system with the energy shifts $\{\epsilon_\alpha\}_\alpha$. When applying (2.22) to a system under study, we determine the densities $\{\langle \hat{n}_\alpha \rangle\}_\alpha$, and thus $\{\epsilon_\alpha\}_\alpha$, of the corresponding reference system *according to* the system under study. In this section, we facilitated the ability to alter the values $\{\epsilon_\alpha\}_\alpha$ and investigate the corresponding densities $\{\langle \hat{n}_\alpha \rangle\}_\alpha$ from the resulting DoS functions $\{f_\alpha(E)\}_\alpha$. Note that since the energy shifts $\{D_\alpha\}_\alpha$ depend on the densities $\{\langle \hat{n}_\alpha \rangle\}_\alpha$, equations (2.26), (2.28) and (2.29) must be solved self-consistently.

Chapter 3

Results

3.1 Local density of states

In this section, we will present results for the DoS functions $\{f_\alpha(E)\}_\alpha$ for one system in accordance with Equation (2.29). Other systems were considered and the results can be found in Appendix C. In all cases presented in this thesis, the systems considered consist of $L = 500$ unit cells (1500 sites) with lattice constant $b = 1$. The chemical potential μ is set to zero by convention and the Dirac delta function is approximated using a Lorentzian according to:

$$\delta(x) \approx \frac{\Gamma}{\pi} \frac{1}{x^2 + \Gamma^2} \tag{3.1}$$

where we set $\Gamma = 0.01$ in the present work. Figure 3.1 shows the resulting DoS functions $\{f_\alpha(E)\}_\alpha$ for a system with energy shifts $\epsilon_c = 0$, $\epsilon_l = -1$ and $\epsilon_r = 1$, for different values of U.

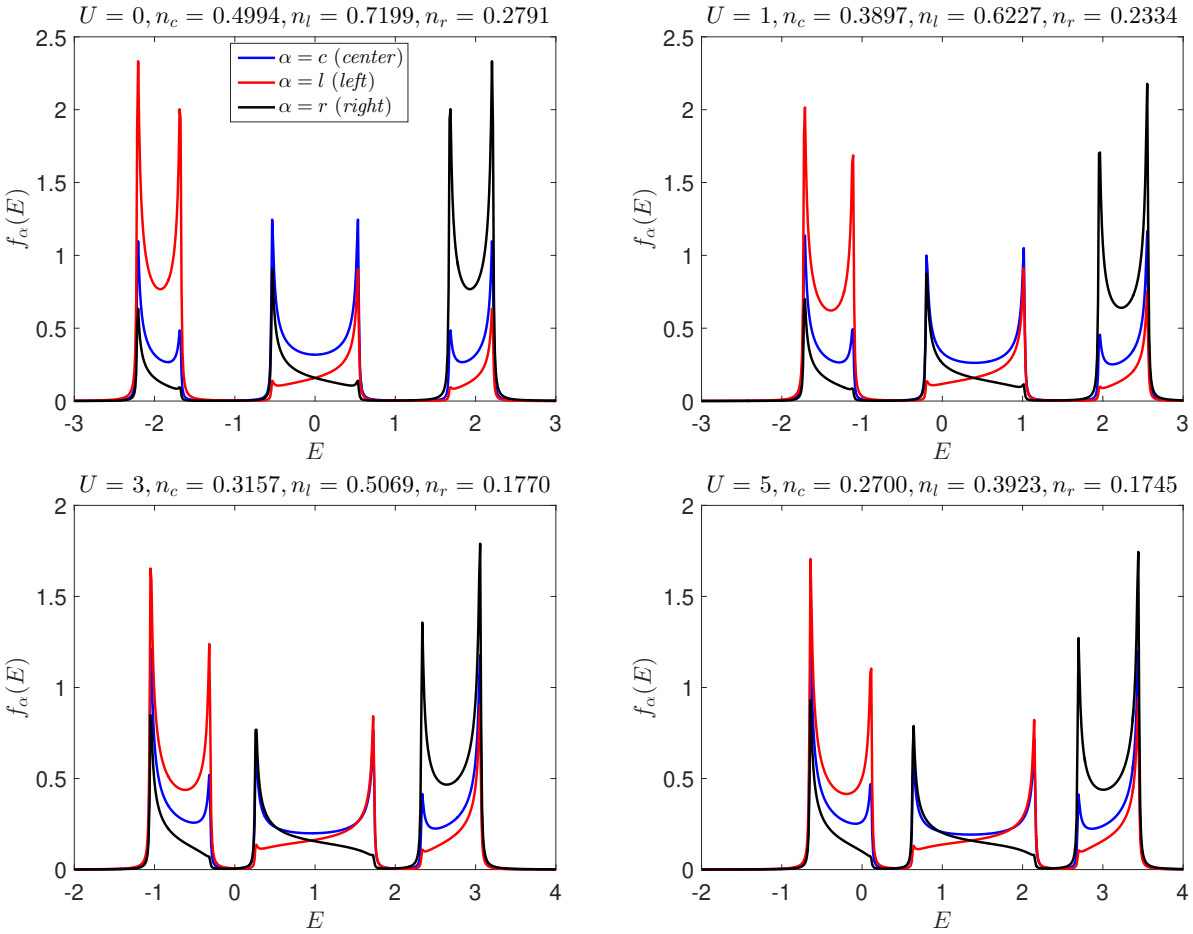

Figure 3.1: Comparison between the density of states functions $\{f_\alpha(E)\}_\alpha$ at four different values of the interaction parameter U, for $\epsilon_c = 0$, $\epsilon_l = -1$ and $\epsilon_r = 1$. Left upper panel: $U = 0$, Right upper panel: $U = 1$, Left lower panel: $U = 3$, Right lower panel: $U = 5$. The densities $\{\langle \hat{n}_\alpha \rangle\}_\alpha$ are also displayed for each case.

If we start by looking at the case of no interaction in Figure 3.1 (Left upper panel), we notice that $f_c(E)$ and the collective graph of $\{f_\alpha(E)\}_\alpha$ are both symmetric around $E = \epsilon_c = 0$. This is a consequence of the symmetry in the unit cell of the system by construction ($\epsilon_l = -1$, $\epsilon_c = 0$ and $\epsilon_r = 1$). Physically, the symmetry of $f_c(E)$ around 0 indicates that the total number of *center* states for $E < \epsilon_c = 0$ is the same as the total number of *center* states for $E > \epsilon_c = 0$ since the absolute difference in energy between ϵ_c and either of ϵ_r and ϵ_l is 1. The total symmetry of $\{f_\alpha(E)\}_\alpha$ around 0 indicates that the total number of states for $E < \epsilon_c = 0$ is the same as the total number of states for $E > \epsilon_c = 0$ which also reflects the symmetry of the unit cell of the system under study. Keeping in mind that the total number of states at one site in the spinless case is 1, these remarks can be confirmed from the values of $\{\langle \hat{n}_\alpha \rangle\}_\alpha$ indicated in Figure 3.1 since we have chosen $\epsilon_c = \mu = 0$.

If we now look at the cases in Figure 3.1 where we have introduced a non-zero interaction parameter U, we notice that in all said cases the collective graph of $\{f_\alpha(E)\}_\alpha$ is shifted to the right (higher energy). This is due to the fact that the interaction introduced is repulsive ($U > 0$) and the resulting energy of said interaction is larger than zero. Therefore, all available energy states are shifted to the right with respect to the case of no interaction. More formally, the local interaction term in the total Hamiltonian of the system adds a diagonal shift to the Hamiltonian of the system without interaction. That is, the system with local interaction can be in first instance be approximately seen as a system without interaction and energy shifts given by: $\epsilon_c' = \epsilon_c + U\langle \hat{n}_c \rangle$, $\epsilon_l' = \epsilon_l + U\langle \hat{n}_l \rangle$ and $\epsilon_r' = \epsilon_r + U\langle \hat{n}_r \rangle$. However, as a consequence of the non-zero interaction parameter U, we also notice a slight asymmetry around ϵ_c' in the cases displayed in Figure 3.1.

The effect of local interaction in Figure 3.1 does not appear to be only a simple shift in $\{f_\alpha(E)\}_\alpha$; in some energy ranges, the shifted graphs become "wider" and "shorter"[1] , e.g. the case of $U = 1$ (Right upper panel) in the energy range $E \in [-0.5, 1.5]$ compared to the case of $U = 0$ (Left upper panel) in the energy range $E \in [-1, 1]$. Mathematically, this is nothing but abiding by the normalization condition, namely, the area under any of the graphs $\{f_\alpha(E)\}_\alpha$ must be 1. Finally, according to Figure 3.1, it is tempting to deduce that the density $\langle \hat{n}_\alpha \rangle$ becomes smaller as U becomes larger. This would be the natural conclusion since if we start adding electrons to the system, we will reach the chemical potential value in energy faster in the case of strongly interacting electrons than not. However, a generalization can not be made, which is evident by the more general case considered in Figure C.1.

[1]By "shorter" we mean that the height of the DoS profile adjusts (being generally reduced) to keep into account normalization requirements.

3.2 Performance of NLA

In this section, we will show the result of employing NLA. We will present a comparison between the performances of LHFA, LSA, CSA and RSA with respect to the exact HF solution for two different systems. The differences between the systems under study will be in the number of sites L, number of electrons N and external perturbation $V_{\text{EXT}} \equiv v_i$ in accordance with equation (2.15). Both systems are studied within the RHF regime ($N_\uparrow = N_\downarrow$). The first external potential we used is the parabolic potential V_p as described by equation (1.18), and the second external potential is a mixed potential V_{mixed} which contains more distortion than V_p and reads:

$$V_{\text{mixed}}(i) = V_p(i) + V_{\text{distortion}}(i) = p(i - \lceil L/2 \rceil)^2 + (i - \lceil L/2 \rceil)e^{-\lambda_1 |i - \lceil L/2 \rceil|} \cos(\lambda_2 (i - \lceil L/2 \rceil)) \quad (3.2)$$

where λ_1 and λ_2 are real numbers. For all results presented in this work, we set: $p = 0.1$, $\lambda_1 = 0.0001$ and $\lambda_2 = 0.3$. The graphs of V_p and V_{mixed} are shown in Figure 3.2.

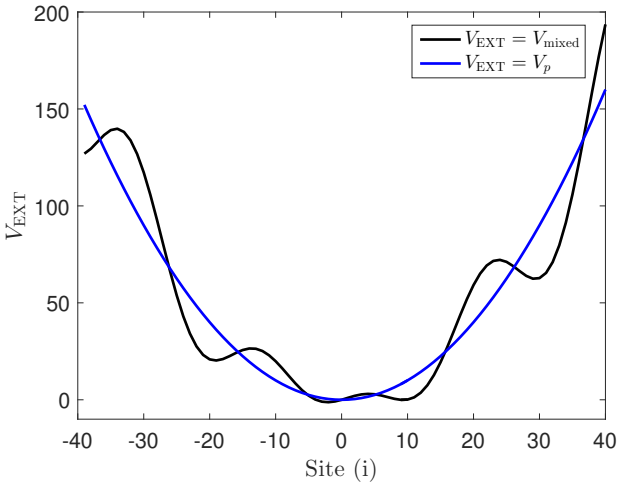

Figure 3.2: Corresponding V_p and V_{mixed} to the set of parameters: $p = 0.1$, $\lambda_1 = 0.0001$ and $\lambda_2 = 0.3$. Note that in this figure, we have used the notation: $\lceil L/2 \rceil \to 0$, positive count for sites to the right of 0 and negative count for sites to the left of 0.

For the long-ranged interaction parameter $U_{ij} = U(|i - j|) = U_k$, the expression used reads as:

$$U_k = \frac{U}{2} \frac{e^{-\lambda_3 k}}{k}, \; k \in \{1, 2, 3, \cdots\} \quad (3.3)$$

where we set $\lambda_3 = 1$ for all cases presented in this thesis. Note that in the following, the higher the local interaction parameter U is, the bigger the effect of the long-ranged interaction in the system considered. First, we present results for a system subjected to the external parabolic potential V_p. Figure 3.3 shows a comparison between all different approximations discussed previously.

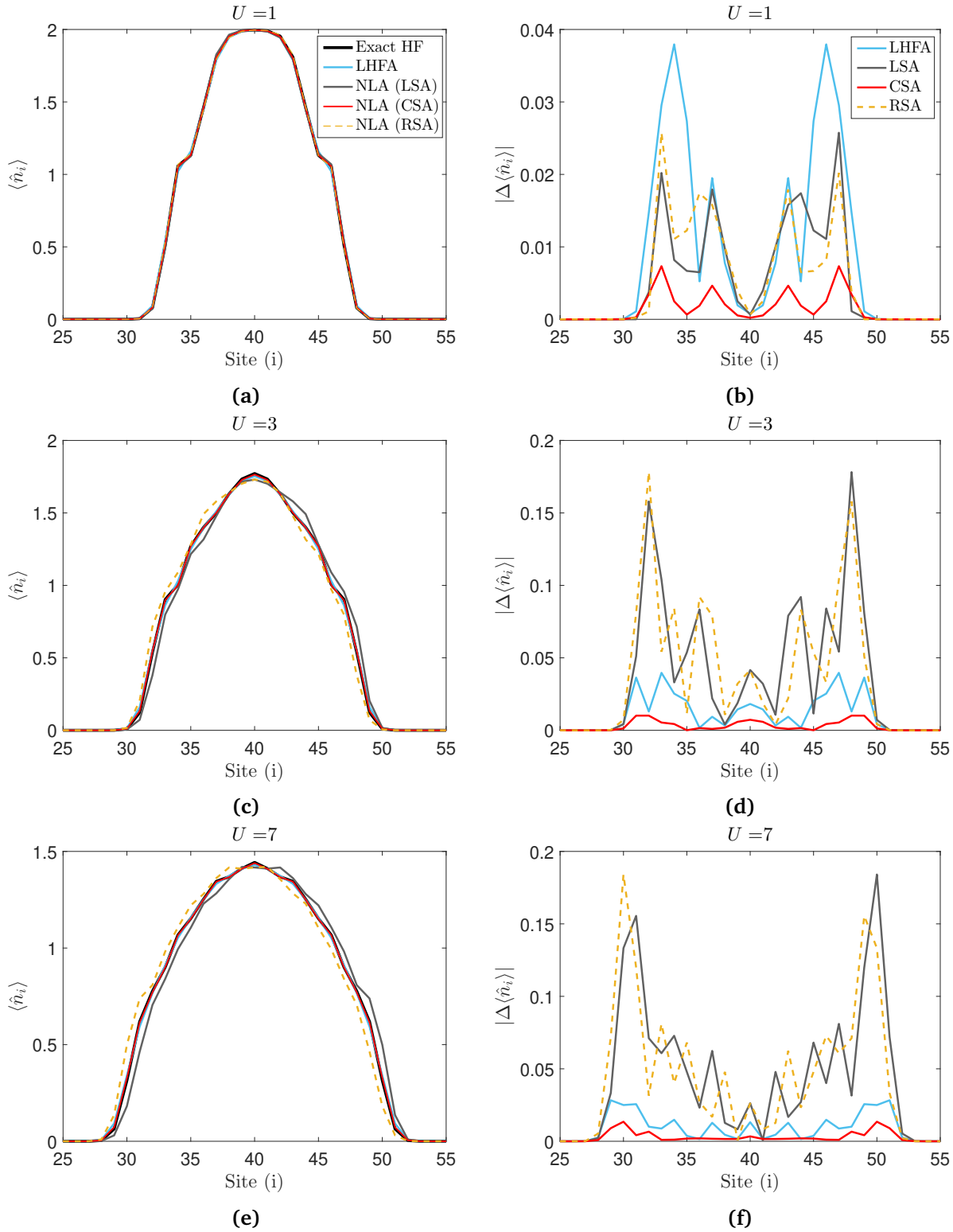

Figure 3.3: Performance of LHFA, LSA, CSA and RSA at different values of the local interaction parameter U, for $L = 80$ sites with $N = 22$ electrons trapped in a parabolic potential V_p. Left panels: density profiles at each value of U, Right panels: performance of each approximation. The quantity used to measure the performance of each approximation is the absolute difference between the exact and approximated densities.

If we start by looking at the case of weak interaction ($U = 1$), Figure 3.3a suggests that all approximations provide a fair description which is more clear in Figure 3.3b where the differences in $|\Delta\langle\hat{n}_i\rangle|$ between all approximations are small (note that the highest value on the y-axis is 0.04). The most interesting aspect in this case is that it is the only case where all variants of NLA perform better than LHFA. However, the *center* site approximation appears to dominate at this point. Looking at the case with medium interaction ($U = 3$), we notice that LSA and RSA fall behind while CSA preserves its superiority over LHFA as shown in Figure 3.3c and Figure 3.3d. Finally, the case of strong interaction ($U = 7$) corroborates its predecessor and concludes that CSA is the best approximation whilst RSA and LSA do not offer any correction over LHFA, rather, they make things worse. This is shown in Figure 3.3e and Figure 3.3f. We notice that the graphs of $|\Delta\langle\hat{n}_i\rangle|$ are even for LHFA and CSA as shown in figures 3.3b, 3.3d and 3.3f which is a result of the symmetry in the external potential, as well as the symmetry of the approximations. However, it is not the case for LSA and RSA, rather, they appear to have a common parity property which will be addressed at the end of this section.

Figure 3.4 shows the same comparison for a different system, however, the external potential used is V_{mixed}. Taking a general look, we immediately notice that no symmetry is observed in figures 3.4b, 3.4d and 3.4f which is a consequence of the distorted potential. Looking at Figure 3.4b, we notice that almost at all sites, RSA and LSA no longer perform better than LHFA as in Figure 3.3b. Although LSA approaches the exact solution at $i = 30$ and predicts the value of $\langle\hat{n}_i\rangle$ closest-to-exact at $i = 35$, the number of sites where LSA and RSA perform well are too few for them to be reliable approximations. In a similar fashion to the previous system, CSA appears to dominate over LHFA according to Figure 3.4b as the number of sites where LHFA performs better than CSA is only one. This is also the case in Figure 3.4d and Figure 3.4f where the number of sites where LHFA outperforms CSA are 4 and 3 respectively (the range of interest is 22 sites). The figures also show a deteriorating performance (especially on the boundaries of the electronic density distribution) of LSA and RSA which confirms our initial conclusion in accordance with Figure 3.4b. Finally, in both systems considered previously, the restriction of the electronic density towards the middle of the lattice is a result of the external potentials, which both exhibits minimas towards the middle of the lattice. This results in electrons being drawn to states with lower energy towards the minimas of the potentials. The effect of interaction is the opposite of this behavior where electrons in the middle of the lattice repel each other and the density profile in the case of interaction has a wider range of sites where the density is non-zero than the case of no interaction.

Looking at the symmetry of the LSA and RSA behavior[2], it is tempting to consider mixing schemes for the densities and/or the potentials. What prevents us from attempting this is that there is no general and conceptually robust guidance of how to choose the mixing, and if doing this on a tentative basis would bring us away from a generic DFT way of thinking. Further elaboration of this point is left for future work.

[2]The density profile produced by LSA is that of RSA with a reflection around the y-axis and vice versa.

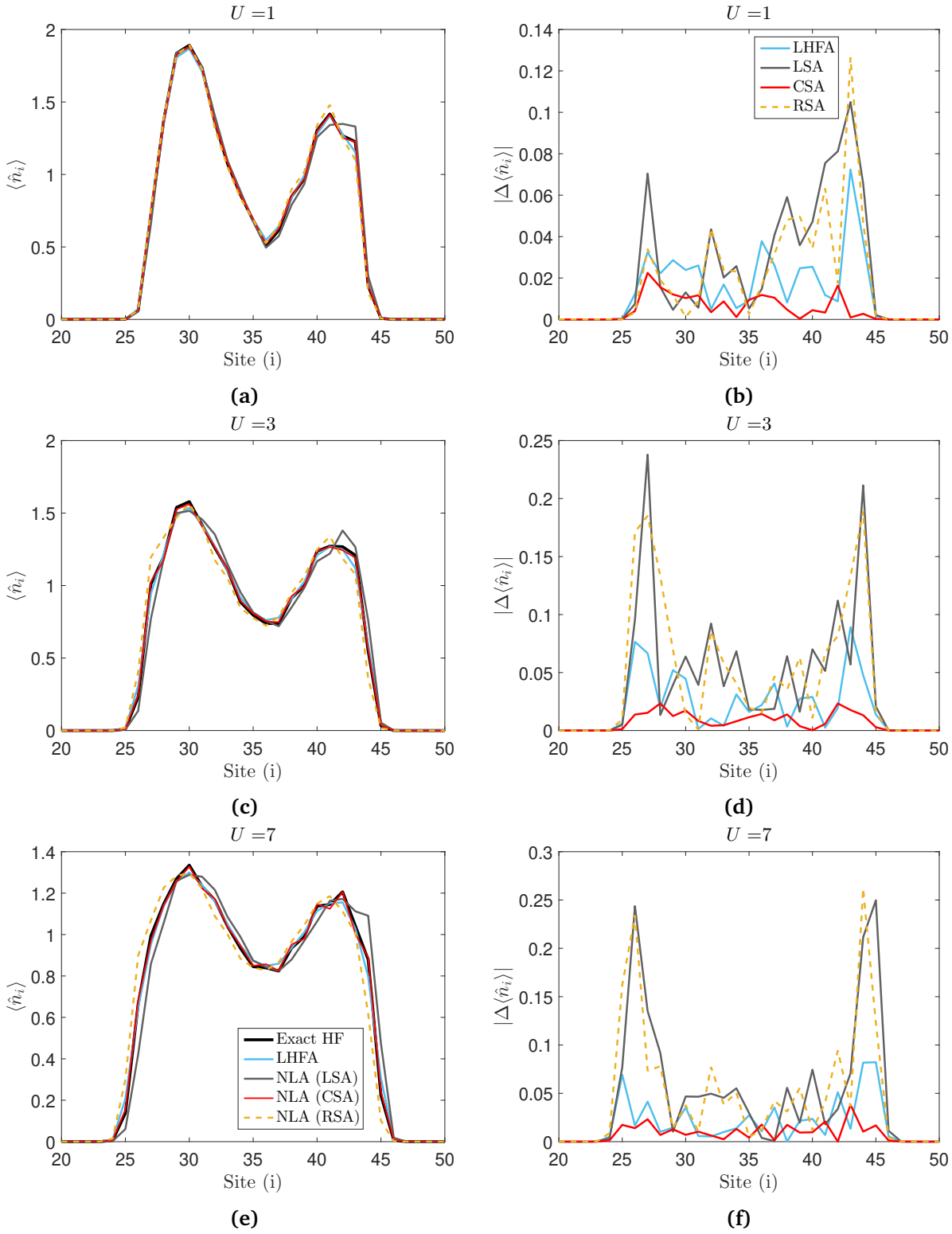

Figure 3.4: Performance of LHFA, LSA, CSA and RSA at different values of the local interaction parameter U, for $L = 64$ sites with $N = 20$ electrons trapped in a mixed potential V_{mixed}. Left panels: density profiles at each value of U, Right panels: performance of each approximation. The quantity used to measure the performance of each approximation is the absolute difference between the exact and approximated densities.

Chapter 4

Conclusions and Outlook

In this thesis, we have developed and tested a near-local approximation for long-ranged electronic interactions in one-dimensional lattice systems. The model we have used is the extended Hubbard model under the Hartree-Fock approximation that accommodates an exponentially decaying long-ranged interaction effect in the presence of an external potential. NLA provided us with three different ways to achieve an approximation based on a reference system that is homogenous up to three consecutive sites, namely LSA, CSA and RSA. All approximations were compared, along with an LDA variant tailored to fit in the HF scheme which we called LHFA, to the exact HF method solution. We have also offered a numerical characterization of the solution for an arbitrary reference system that is homogenous up to three consecutive sites in the case of local interaction only by studying the DoS in a unit cell of the reference system.

In the case of an external parabolic potential, we have found that at low interaction all variants of NLA outperform LHFA, however, at any case of stronger interaction the performances of LSA and RSA are lacking. Albeit LSA and RSA fall behind dramatically (specifically on the boundaries), our results suggest that CSA *always* performs better than LHFA. For an external potential with a degree of disorder, we have found that the situation is not changed greatly compared to that of its predecessor. The results we have presented indicate a deteriorating performance of LSA and RSA with increased interaction. Furthermore, LHFA outperforms CSA at a few number of sites, nevertheless, CSA remains the best approximation. This leads us to conclude that a near-local treatment can in fact produce better results than a local one which opens the door for a more thorough and accurate implementation of NLA in the future.

In this respect, the next step would be to explicitly consider correlation effects in a 1D reference system with a 3-site supercell, where the densities inside the cell are varied independently to produce an exchange-correlation term $E_{xc}(\langle\hat{n}_l\rangle, \langle\hat{n}_c\rangle, \langle\hat{n}_r\rangle)$. Differently from the fully homogenous 1D Hubbard model, there is no exact analytical solution for this case, and numerical methods as e.g. density matrix renormalization group (DMRG) [22] should thus be considered. Alternatively, correlation effects could be introduced in a perturbative way. Through many-body perturbation theory, it is possible to consider approximations of increasing complexity and with them to compute the total energy, from which E_{xc} (and thus V_{xc}) would be extracted. In this case, already a simple 1D system with on-site-only interaction, and correlations treated in a low-level description such as second Born [23], would be enough to further test and qualitatively validate the effectiveness of our proposal of a near-local approximation.

References

[1] P. Hohenberg and W. Kohn. “Inhomogeneous electron gas.” *Physical review* 136.3B (1964): B864.

[2] J. Hubbard. “Electron correlations in narrow energy bands.” *Proc. R. Soc. Lond. A.* Vol. 276. No. 1365. The Royal Society, (1963).

[3] W. Kohn and L. Sham. “Self-consistent equations including exchange and correlation effects.” *Physical review* 140.4A (1965): A1133.

[4] R. G. Parr and W. Yang. *Density Functional Theory of Atoms and Molecules*. Oxford: OUP, (1989).

[5] W. Koch and M. C. Holthausen. *A Chemist’s Guide to Density Functional Theory* (2nd edition). Wiley-VCH Verlag GmbH, (2001).

[6] K. Schönhammer, O. Gunnarsson, and R.M. Noack. “Density-functional theory on a lattice: Comparison with exact numerical results for a model with strongly correlated electrons.” *Physical review* 52.4B (1995): 2504.

[7] O. Gunnarsson and K. Schönhammer. “Density-functional treatment of an exactly solvable semiconductor model.” *Physical review letters* 56.18 (1986): 1968.

[8] E. H. Lieb and F. Y. Wu. “Absence of Mott transition in an exact solution of the shortrange, one-band model in one dimension.” *Physical review letters* 20.25 (1964): 1445.

[9] N. A. Lima, M. F. Silva, L. N. Oliveira and K. Capelle. “Density-functionals not based on the electron gas: Local-density approximation for a Luttinger liquid.” *Physical review letters* 90.14 (2003): 146402.

[10] C. Verdozzi. “Lieb’s solution and Capelle’s DFT in short: their use in TDDFT-ALDA.” *Unpublished report*.

[11] H. Bruus and K. Flensberg. *Many-body quantum theory in condensed matter physics: an introduction*. Oxford university press, (2004).

[12] E. Pavarini, et al. *The LDA+DMFT approach to strongly correlated materials*. No. PreJuSER-17645. Theoretische Nanoelektronik, (2011).

[13] F. H. Essler, et al. *The one-dimensional Hubbard model*. Cambridge University Press, (2005).

[14] D. R. Hartree. “The wave mechanics of an atom with a non-Coulomb central field. Part I. Theory and methods.” *Mathematical Proceedings of the Cambridge Philosophical Society.* Vol. 24. No. 1. Cambridge University Press, (1928).

[15] D. R. Hartree, F.R.S. and W. Hartree. “Self-consistent field, with exchange, for beryllium.” *Proc. R. Soc. Lond. A.* 150.869 (1935): 9-33.

[16] J. C. Slater. “The self consistent field and the structure of atoms.” *Physical Review* 32.3 (1928): 339.

[17] V. Fock. “Näherungsmethode zur Lösung des quantenmechanischen Mehrkörperproblems.” *Zeitschrift für Physik* 61.1-2 (1930): 126-148.

[18] J. A. Gaunt. “A Theory of Hartree’s Atomic Fields.” *Mathematical Proceedings of the Cambridge Philosophical Society.* Vol. 24. No. 2. Cambridge University Press, (1928).

[19] A. Szabo and N. S. Ostlund. *Modern Quantum Chemistry: Intro to Advanced Electronic Structure Theory.* (1996).

[20] K. Capelle and V. L. Campo Jr. “Density functionals and model Hamiltonians: Pillars of many-particle physics.” *Physics Reports* 528.3 (2013): 91-159.

[21] K. Schönhammer and O. Gunnarsson. “Discontinuity of the exchange-correlation potential in density functional theory.” *Journal of Physics C: Solid State Physics* 20.24 (1987): 3675.

[22] G. De Chiara, et al. “Density matrix renormalization group for dummies.” *Journal of Computational and Theoretical Nanoscience* 5.7 (2008): 1277-1288.

[23] A. L. Fetter and J. D. Walecka. *Quantum theory of many-particle systems.* Courier Corporation, (2012).

[24] J. C. Slater. “A simplification of the Hartree-Fock method.” *Physical Review* 81.3 (1951): 385.

[25] D. M. Ceperley and B. J Alder. “Ground state of the electron gas by a stochastic method.” *Physical Review Letters* 45.7 (1980): 566.

Appendix A

Notation

The following notations are used throughout this thesis unless stated otherwise. Boldface uppercase denote matrices (e.g. $\boldsymbol{A}$), boldface lowercase denote vectors (e.g. $\mathbf{a}$) and standard letters denote scalars (e.g. a). By $\mathbf{x}$ we will always mean a four-dimensional vector that consists of the 3-dimensional spatial vector $\mathbf{r}$ and a spin coordinate $s \in \{\uparrow, \downarrow\}$. $\uparrow$ denotes spin-up and $\downarrow$ denotes spin-down. $\dfrac{\delta}{\delta f(x)}$ denotes the variational derivative with respect to $f(x)$. $\mathrm{eig}(\boldsymbol{A})$ denotes the set of eigenvalues of the matrix $\boldsymbol{A}$ and $\mathrm{diag}(a_1, a_2, a_3, \cdots, a_n)$ denotes a diagonal matrix (with dimensions made clear from the context) with diagonal entries $\{a_1, a_2, a_3, \cdots, a_n\}$. $(\cdot)^*$ denotes complex conjugation. $\hat{(\cdot)}$ denotes an operator and $\mathbb{1}$ denotes the identity operator. $(\hat{\cdot})^\dagger$ and $\langle(\hat{\cdot})\rangle$ denote the conjugate transpose (Hermitian conjugate) and the expectation value of an operator respectively. δ_{ij} denotes the Kronecker delta and $\delta(x)$ denotes the Dirac delta function centered at $x = 0$. By the symbol L we will always mean the number of unit cells or number of sites depending on the context whether finite or infinite. Summations or counts taken over non-specified indices should have an upper limit of L where appropriate. Finally, we shall adapt the following abbreviation:

$$\det\{\aleph_1(\mathbf{x}_1)\aleph_2(\mathbf{x}_2)\cdots\aleph_N(\mathbf{x}_N)\} \equiv \begin{vmatrix} \aleph_1(\mathbf{x}_1) & \aleph_2(\mathbf{x}_1) & \dots & \aleph_N(\mathbf{x}_1) \\ \aleph_1(\mathbf{x}_2) & \aleph_2(\mathbf{x}_2) & \dots & \aleph_N(\mathbf{x}_2) \\ \vdots & \vdots & \ddots & \vdots \\ \aleph_1(\mathbf{x}_N) & \aleph_2(\mathbf{x}_N) & \dots & \aleph_N(\mathbf{x}_N) \end{vmatrix}. \tag{A.1}$$

Appendix B

Derivations

A derivation of Approximation 2: Additional details

We start from equation (2.21). After expanding the summation over α' and replacing $\langle \hat{n}_{j'\alpha'} \rangle$ by $\langle \hat{n}_{\alpha'} \rangle$ since it is independent of the unit cell index j' by construction, we get:

$$V_{j\alpha}^{\text{NLA}} = \sum_{j'} \left[U_{j\alpha j' l}(1 - \delta_{jj'}\delta_{\alpha l})\langle \hat{n}_l \rangle + U_{j\alpha j' c}(1 - \delta_{jj'}\delta_{\alpha c})\langle \hat{n}_c \rangle + U_{j\alpha j' r}(1 - \delta_{jj'}\delta_{\alpha r})\langle \hat{n}_r \rangle \right]. \tag{B.1}$$

If we now choose α=l, i.e. we want to find the potential felt at the *left* site of an arbitrary unit cell j, we get:

$$\begin{aligned} V_{jl}^{\text{NLA}} &= \sum_{j'} \left[U_{jlj' l}(1 - \delta_{jj'}\delta_{ll})\langle \hat{n}_l \rangle + U_{jlj' c}(1 - \delta_{jj'}\delta_{lc})\langle \hat{n}_c \rangle + U_{jlj' r}(1 - \delta_{jj'}\delta_{lr})\langle \hat{n}_r \rangle \right] \\ &= \sum_{j'} \left[U_{jlj' l}(1 - \delta_{jj'})\langle \hat{n}_l \rangle + U_{jlj' c}\langle \hat{n}_c \rangle + U_{jlj' r}\langle \hat{n}_r \rangle \right]. \end{aligned} \tag{B.2}$$

Since the reference system is infinite, there are infinite unit cells to the left and right of j. If we start the summation in equation (B.2) from $j' = j$ and expand to the left and right of j in a similar fashion to what we did in the case of LHFA, we get:

$$\begin{aligned} V_{jl}^{\text{NLA}} = \big[& U_{jljl}(1 - \delta_{jj})\langle \hat{n}_l \rangle + U_{jljc}\langle \hat{n}_c \rangle + U_{jljr}\langle \hat{n}_r \rangle \\ & + U_{jl(j+1)l}(1 - \delta_{j(j+1)})\langle \hat{n}_l \rangle + U_{jl(j+1)c}\langle \hat{n}_c \rangle + U_{jl(j+1)r}\langle \hat{n}_r \rangle \\ & + U_{jl(j+2)l}(1 - \delta_{j(j+2)})\langle \hat{n}_l \rangle + U_{jl(j+2)c}\langle \hat{n}_c \rangle + U_{jl(j+2)r}\langle \hat{n}_r \rangle \\ & + U_{jl(j-1)l}(1 - \delta_{j(j-1)})\langle \hat{n}_l \rangle + U_{jl(j-1)c}\langle \hat{n}_c \rangle + U_{jl(j-1)r}\langle \hat{n}_r \rangle \\ & + U_{jl(j-2)l}(1 - \delta_{j(j-2)})\langle \hat{n}_l \rangle + U_{jl(j-2)c}\langle \hat{n}_c \rangle + U_{jl(j-2)r}\langle \hat{n}_r \rangle \\ & + \ldots \big]. \end{aligned} \tag{B.3}$$

If we further assume, as in the case of LHFA, that $U_{j\alpha j'\alpha'} = U(k) = U_k$ where k denotes the distance between the sites $j\alpha$ and $j'\alpha'$ (k=1 for consecutive sites), the above equation reads:

$$\begin{aligned} V_{jl}^{\text{NLA}} = & \underbrace{\left[U_1\langle \hat{n}_c \rangle + U_2\langle \hat{n}_r \rangle + U_3\langle \hat{n}_l \rangle + U_4\langle \hat{n}_c \rangle + U_5\langle \hat{n}_r \rangle + U_6\langle \hat{n}_l \rangle + U_7\langle \hat{n}_c \rangle + U_8\langle \hat{n}_r \rangle + \ldots \right]}_{\text{right of } j} \\ & + \underbrace{\left[U_3\langle \hat{n}_l \rangle + U_2\langle \hat{n}_c \rangle + U_1\langle \hat{n}_r \rangle + U_6\langle \hat{n}_l \rangle + U_5\langle \hat{n}_c \rangle + U_4\langle \hat{n}_r \rangle + \ldots \right]}_{\text{left of } j}. \end{aligned} \tag{B.4}$$

Figure B.1 shows an illustration of equation (B.4), which after rearrangement reads:

$$\begin{aligned} V_{jl}^{\text{NLA}} &= U_1(\langle\hat{n}_c\rangle + \langle\hat{n}_r\rangle) + U_2(\langle\hat{n}_c\rangle + \langle\hat{n}_r\rangle) + 2U_3\langle\hat{n}_l\rangle \\ &+ U_4(\langle\hat{n}_c\rangle + \langle\hat{n}_r\rangle) + U_5(\langle\hat{n}_c\rangle + \langle\hat{n}_r\rangle) + 2U_6\langle\hat{n}_l\rangle \\ &+ U_7\langle\hat{n}_c\rangle + U_8\langle\hat{n}_r\rangle + \ldots \\ &= \sum_{k=1}^{\infty} U_k(\langle\hat{n}_c\rangle + \langle\hat{n}_r\rangle)(1 - \delta_{0\text{mod}(k,3)}) + 2\sum_{k=1}^{\infty} U_k\langle\hat{n}_l\rangle\delta_{0\text{mod}(k,3)} \end{aligned} \tag{B.5}$$

where $\text{mod}(k,3) = 0$ if $k/3$ is an integer and non-zero otherwise which is known as the modulus (or modulo) arithmetic operation. Further rearrangement after adding and subtracting the quantity $\sum_{k=1}^{\infty} U_k\langle\hat{n}_l\rangle(1 - \delta_{0\text{mod}(k,3)})$ would yield the final result for V_{jl}^{NLA} given by:

$$V_{jl}^{\text{NLA}} = \langle\hat{n}_{\text{cell}}\rangle \sum_{k=1}^{\infty} U_k(1 - \delta_{0\text{mod}(k,3)}) + \langle\hat{n}_l\rangle \sum_{k=1}^{\infty}(3U_{3k} - U_k) \tag{B.6}$$

where $\langle\hat{n}_{\text{cell}}\rangle = \langle\hat{n}_l + \hat{n}_c + \hat{n}_r\rangle = \langle\hat{n}_l\rangle + \langle\hat{n}_c\rangle + \langle\hat{n}_r\rangle$. Equation (B.6) holds in general, that is, whether we chose the *left*, *center* or *right* site the expression remains analogous to that of V_{jl}^{NLA}. It can be shown by direct calculation that for $\alpha \in \{l, c, r\}$, we have:

$$V_{j\alpha}^{\text{NLA}} = \langle\hat{n}_{\text{cell}}\rangle \sum_{k=1}^{\infty} U_k(1 - \delta_{0\text{mod}(k,3)}) + \langle\hat{n}_\alpha\rangle \sum_{k=1}^{\infty}(3U_{3k} - U_k). \tag{B.7}$$

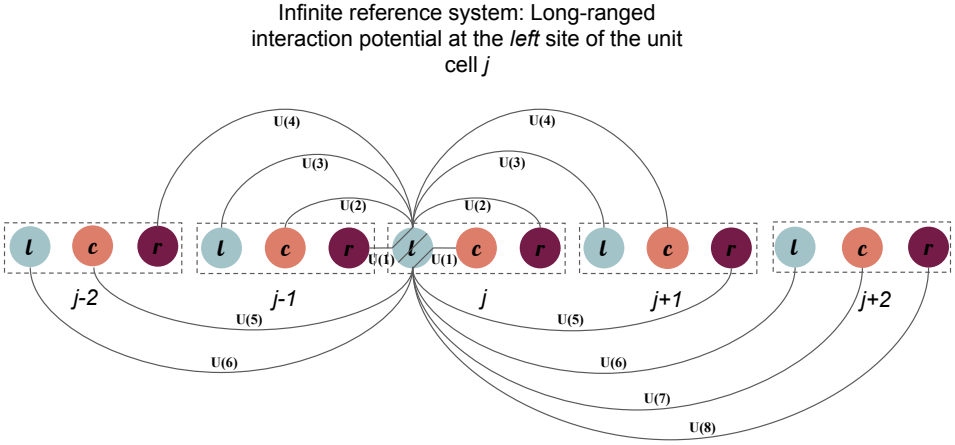

Figure B.1: A sketch that shows the contribution of neighboring sites to the long-ranged interaction potential at the *left* site of the unit cell j. Note that the lattice is infinite and the figure only shows the nearest and second nearest neighboring unit cells to the unit cell j.

The lingering $\alpha \in \{l, c, r\}$ degree of freedom in $V_{j\alpha}^{\text{NLA}}$ is problematic for extracting an approximation for V_i from such reference system. For a system under study that has inherently a degree of homogeneity similar to that of the reference system we used, the problem is avoided by dividing the system under study to unit cells in the same manner as we have done for the reference system. The approximation for V_i can be readily used in accordance with equation (B.7). However, most realistic systems we are interested in have not any degree of homogeneity. In fact, a simple

parabolic potential (which is vastly used to study trapped ultra-cold atoms) would get rid of any translational symmetry of the problem at hand.

In the most general case where $\langle \hat{n}_j \rangle \neq \langle \hat{n}_{j'} \rangle$ when $j \neq j'$ (here j and j' are site indices) for the system under study, we can choose to treat any arbitrary site i as either a *left*, *center* or *right* site in a corresponding reference system with the corresponding approximation given by equation (B.7). The mapping between the density at site i and the corresponding reference system is no longer unique due to the approximation depending on the density at an extra pair of sites neighboring i. In fact, by virtue of the expression given by equation (B.7) for $V_{j\alpha}^{\text{NLA}}$, there are exactly three possible approximations extracted from three possible reference systems having the degree of homogeneity as mentioned above. The reference systems, and therefore the approximations, differ from each other in the value of $\langle \hat{n}_{\text{cell}} \rangle$. If we choose the site i to be a *left* site, then $\langle \hat{n}_{\text{cell}} \rangle = \langle \hat{n}_i \rangle + \langle \hat{n}_{i+1} \rangle + \langle \hat{n}_{i+2} \rangle$ and so on, giving a *left* site approximation, a *center* site approximation and a *right* site approximation. This is illustrated in Figure 2.2. Finally, taking all possible approximations into account, we get A 2. □

A derivation of Equation (2.25)

We start by writing the tight-binding Hamiltonian in the lattice-site single particle states $\{|j\rangle\}_j$, we get:

$$\hat{H}_{\text{TB}} = -t\sum_{\langle i,j\rangle}\hat{c}_i^\dagger\hat{c}_j = -t\sum_j(\hat{c}_j^\dagger\hat{c}_{j+1} + \hat{c}_{j+1}^\dagger\hat{c}_j) = -t\sum_j(|j\rangle\langle j+1| + |j+1\rangle\langle j|). \tag{B.8}$$

According to Bloch's theorem, the k states $\{|k\rangle\}_j$ are given by:

$$|k\rangle = \frac{1}{\sqrt{L}}\sum_j e^{ikj}|j\rangle \tag{B.9}$$

where L is the number of unit cells. If we now use the above equations to calculate the matrix elements of $\hat{H}_{\text{TB}}$ in the basis $\{|k\rangle\}_j$, we get:

$$\begin{aligned}
\langle k'|\hat{H}_{\text{TB}}|k\rangle &= -t\frac{1}{\sqrt{L}}\sum_n e^{-ik'n}\langle n|\sum_j(|j\rangle\langle j+1| + |j+1\rangle\langle j|)\frac{1}{\sqrt{L}}\sum_m e^{ikm}|m\rangle \\
&= -t\frac{1}{L}\sum_j\Big[\sum_n e^{-ik'n}\langle n|j\rangle\sum_m e^{ikm}\langle j+1|m\rangle + \sum_n e^{-ik'n}\langle n|j+1\rangle\sum_m e^{ikm}\langle j|m\rangle\Big] \\
&= -t\frac{1}{L}\sum_j(e^{-ik'j}e^{ik(j+1)} + e^{-ik'(j+1)}e^{ikj}) = -te^{ik}\frac{1}{L}\sum_j e^{i(k-k')j} - te^{-ik'}\frac{1}{L}\sum_j e^{i(k-k')j}
\end{aligned} \tag{B.10}$$

where we have used the fact that the states $\{|j\rangle\}_j$ constitute a complete basis. Finally, using the identity:

$$\frac{1}{L}\sum_j e^{i(k-k')j} = \delta_{kk'} \tag{B.11}$$

(B.10) reads:

$$\langle k'|\hat{H}_{\text{TB}}|k\rangle = -t\delta_{kk'}(e^{ik} + e^{-ik'}) = \begin{cases} -t(e^{ik} + e^{-ik}) = -2t\cos k & k = k' \\ 0 & k \neq k' \end{cases} \tag{B.12}$$

which indicates that the matrix for $\hat{H}_{\text{TB}}$ in the basis $\{|k\rangle\}_j$ is diagonal. In other words, the states $\{|k\rangle\}_j$ are eigenstates of $\hat{H}_{\text{TB}}$ and the energy values allowed are the eigenvalues of the matrix representing $\hat{H}_{\text{TB}}$. The eigenvalues of a diagonal matrix are simply the entries of the diagonal of the matrix, that is, the matrix elements $\langle k|\hat{H}_{\text{TB}}|k\rangle$ which completes the proof. □

A derivation of Statement 1

Let the lattice-site single particle states be denoted by $\{|j\alpha\rangle\}_{j\alpha}$ where $\alpha \in \{c, l, r\}$ and construct the single particle states $\{|k_p\alpha\rangle\}_{p\alpha}$ where for a given, yet arbitrary, $k_p = k$ we have[1]:

$$\begin{aligned} |kl\rangle &= \frac{1}{\sqrt{L}} \sum_j e^{ikj} |jl\rangle \\ |kc\rangle &= \frac{1}{\sqrt{L}} \sum_j e^{ikj} |jc\rangle \\ |kr\rangle &= \frac{1}{\sqrt{L}} \sum_j e^{ikj} |jr\rangle. \end{aligned} \tag{B.13}$$

This is in accordance with the periodic boundary conditions and conservation of the total particle (states) number. Namely, the number of k states is the same as the number of unit cells L, and the number of single particle states is $3L$, which is the number of lattice sites where each site accommodates at most one electron in the spinless case. The Bloch states given by (B.13) are not guaranteed to be energy eigenstates in general. This is evident by the quantum number α which holds information about the position, therefore, the states $\{|k\alpha\rangle\}_\alpha$ are not purely k states. The summation in the tight-binding Hamiltonian $\hat{H}^{\text{ref}}_{\text{TB}}$ as given in (2.23) is over ordered pairs $\langle j\alpha, j'\alpha'\rangle$ and thus, unlike the one-dimensional homogenous Hubbard model, hopping inside the same unit cell with index j (or j') is allowed. After expanding the summations over α and α', the Hamiltonian $\hat{H}^{\text{ref}}_{\text{HF}}$ in (2.23) reads:

$$\begin{aligned} \hat{H}^{\text{ref}}_{\text{HF}} = &- t \sum_j (\hat{c}^\dagger_{jc}\hat{c}_{jr} + \hat{c}^\dagger_{jr}\hat{c}_{jc} + \hat{c}^\dagger_{jc}\hat{c}_{jl} + \hat{c}^\dagger_{jl}\hat{c}_{jc} + \hat{c}^\dagger_{jr}\hat{c}_{(j+1)l} + \hat{c}^\dagger_{(j+1)l}\hat{c}_{jr}) \\ &+ \sum_j \left[(\epsilon_c + Un_{jc})\hat{n}_{jc} + (\epsilon_l + Un_{jl})\hat{n}_{jl} + (\epsilon_r + Un_{jr})\hat{n}_{jr} \right]. \end{aligned} \tag{B.14}$$

If we furthermore write $\hat{H}^{\text{ref}}_{\text{HF}}$ in terms of the single particle states $\{|j\alpha\rangle\}_{j\alpha}$ we get:

$$\begin{aligned} \hat{H}^{\text{ref}}_{\text{HF}} = &- t \sum_j (|jc\rangle\langle jr| + |jr\rangle\langle jc| + |jc\rangle\langle jl| + |jl\rangle\langle jc| + |jr\rangle\langle (j+1)l| + |(j+1)l\rangle\langle jr|) \\ &+ \sum_j \left[(\epsilon_c + Un_{jc})|jc\rangle\langle jc| + (\epsilon_l + Un_{jl})|jl\rangle\langle jl| + (\epsilon_r + Un_{jr})|jr\rangle\langle jr| \right]. \end{aligned} \tag{B.15}$$

From (B.13), we have:

$$\begin{aligned} |k\alpha\rangle &= \frac{1}{\sqrt{L}} \sum_m e^{ikm} |m\alpha\rangle \\ \langle k'\alpha'| &= \frac{1}{\sqrt{L}} \sum_{m'} e^{-ik'm'} \langle m'\alpha'|. \end{aligned} \tag{B.16}$$

[1] In this proof, we will adapt the notation $\langle\hat{n}\rangle = n$ to make it easier to read.

Evaluating the matrix elements $\langle k'\alpha'|\hat{H}^{\text{ref}}_{\text{HF}}|k\alpha\rangle$ using (B.15) and (B.16), we get:

$$
\begin{aligned}
\langle k'\alpha'|\hat{H}^{\text{ref}}_{\text{HF}}|k\alpha\rangle = -\frac{t}{L}\sum_j \Big[& \sum_{m'} e^{-ik'm'}\langle m'\alpha'|jc\rangle \sum_m e^{ikm}\langle jr|m\alpha\rangle \\
& + \sum_{m'} e^{-ik'm'}\langle m'\alpha'|jr\rangle \sum_m e^{ikm}\langle jc|m\alpha\rangle \\
& + \sum_{m'} e^{-ik'm'}\langle m'\alpha'|jc\rangle \sum_m e^{ikm}\langle jl|m\alpha\rangle \\
& + \sum_{m'} e^{-ik'm'}\langle m'\alpha'|jl\rangle \sum_m e^{ikm}\langle jc|m\alpha\rangle \\
& + \sum_{m'} e^{-ik'm'}\langle m'\alpha'|jr\rangle \sum_m e^{ikm}\langle (j+1)l|m\alpha\rangle \\
& + \sum_{m'} e^{-ik'm'}\langle m'\alpha'|(j+1)l\rangle \sum_m e^{ikm}\langle jr|m\alpha\rangle \Big] \\
+\frac{1}{L}\sum_j \Big[& (\epsilon_c + Un_{jc}) \sum_{m'} e^{-ik'm'}\langle m'\alpha'|jc\rangle \sum_m e^{ikm}\langle jc|m\alpha\rangle \\
& + (\epsilon_l + Un_{jl}) \sum_{m'} e^{-ik'm'}\langle m'\alpha'|jl\rangle \sum_m e^{ikm}\langle jl|m\alpha\rangle \\
& + (\epsilon_r + Un_{jr}) \sum_{m'} e^{-ik'm'}\langle m'\alpha'|jr\rangle \sum_m e^{ikm}\langle jr|m\alpha\rangle \Big] \\
= -\frac{t}{L}\sum_j \Big[& e^{-ik'j}\langle j\alpha'|jc\rangle e^{ikj}\langle jr|j\alpha\rangle + e^{-ik'j}\langle j\alpha'|jr\rangle e^{ikj}\langle jc|j\alpha\rangle \\
& + e^{-ik'j}\langle j\alpha'|jc\rangle e^{ikj}\langle jl|j\alpha\rangle + e^{-ik'j}\langle j\alpha'|jl\rangle e^{ikj}\langle jc|j\alpha\rangle \\
& + e^{-ik'j}\langle j\alpha'|jr\rangle e^{ik(j+1)}\langle (j+1)l|(j+1)\alpha\rangle \\
& + e^{-ik'(j+1)}\langle (j+1)\alpha'|(j+1)l\rangle e^{ikj}\langle jr|j\alpha\rangle \Big] \\
+\frac{1}{L}\sum_j \Big[& (\epsilon_c + Un_{jc}) e^{-ik'j}\langle j\alpha'|jc\rangle e^{ikj}\langle jc|j\alpha\rangle \\
& + (\epsilon_l + Un_{jl}) e^{-ik'j}\langle j\alpha'|jl\rangle\ e^{ikj}\langle jl|j\alpha\rangle \\
& + (\epsilon_r + Un_{jr}) e^{-ik'j}\langle j\alpha'|jr\rangle e^{ikj}\langle jr|j\alpha\rangle \Big] \\
= -\frac{t}{L}\sum_j e^{i(k-k')j}\Big[& \langle j\alpha'|jc\rangle\langle jr|j\alpha\rangle + \langle j\alpha'|jr\rangle\langle jc|j\alpha\rangle \\
& + \langle j\alpha'|jc\rangle\langle jl|j\alpha\rangle + \langle j\alpha'|jl\rangle\langle jc|j\alpha\rangle \\
& + e^{ik}\langle j\alpha'|jr\rangle\langle (j+1)l|(j+1)\alpha\rangle \\
& + e^{-ik'}\langle (j+1)\alpha'|(j+1)l\rangle\langle jr|j\alpha\rangle \Big] \\
+\frac{1}{L}\sum_j e^{i(k-k')j}\Big[& (\epsilon_c + Un_{jc})\langle j\alpha'|jc\rangle\langle jc|j\alpha\rangle \\
& + (\epsilon_l + Un_{jl})\langle j\alpha'|jl\rangle\ \langle jl|j\alpha\rangle \\
& + (\epsilon_r + Un_{jr})\langle j\alpha'|jr\rangle\langle jr|j\alpha\rangle \Big]
\end{aligned}
$$

where the completeness of the basis $\{|j\alpha\rangle\}_{j\alpha}$ was used in the second equality. According to above calculations, the matrix elements for $\hat{H}^{\text{ref}}_{\text{HF}}$ are given by:

$$\langle k'\alpha'|\hat{H}^{\text{ref}}_{\text{HF}}|k\alpha\rangle = \frac{1}{L}\sum_j e^{i(k-k')j}(P+Q) \tag{B.17}$$

where P and Q are defined as:

$$\begin{aligned} P \equiv -t\big[&\langle j\alpha'|jc\rangle\langle jr|j\alpha\rangle + \langle j\alpha'|jr\rangle\langle jc|j\alpha\rangle + \langle j\alpha'|jc\rangle\langle jl|j\alpha\rangle + \langle j\alpha'|jl\rangle\langle jc|j\alpha\rangle \\ &+ e^{ik}\langle j\alpha'|jr\rangle\langle (j+1)l|(j+1)\alpha\rangle + e^{-ik'}\langle (j+1)\alpha'|(j+1)l\rangle\langle jr|j\alpha\rangle\big] \\ Q \equiv (\epsilon_c + Un_{jc})&\langle j\alpha'|jc\rangle\langle jc|j\alpha\rangle + (\epsilon_l + Un_{jl})\langle j\alpha'|jl\rangle\ \langle jl|j\alpha\rangle + (\epsilon_r + Un_{jr})\langle j\alpha'|jr\rangle\langle jr|j\alpha\rangle. \end{aligned} \tag{B.18}$$

Given the completeness of $\{|j\alpha\rangle\}_{j\alpha}$, it is easy to check that the following relations hold:

$$\begin{aligned} &P(\alpha' = \alpha) = 0 \\ &Q(\alpha' = \alpha) = \epsilon_\alpha + Un_{j\alpha} \\ &P(\alpha' \neq \alpha) = \begin{cases} -te^{ik} & \alpha' = r \text{ and } \alpha = l \\ -te^{-ik'} & \alpha' = l \text{ and } \alpha = r \\ -t & \text{otherwise} \end{cases} \\ &Q(\alpha' \neq \alpha) = 0. \end{aligned} \tag{B.19}$$

Using (B.17), (B.19) and (B.11) , the matrix elements for $\hat{H}^{\text{ref}}_{\text{HF}}$ can be written as:

$$\begin{aligned} \langle k'\alpha'|\hat{H}^{\text{ref}}_{\text{HF}}|k\alpha\rangle &= \begin{cases} (\epsilon_\alpha + Un_{j\alpha})\frac{1}{L}\sum_j e^{i(k-k')j} = (\epsilon_\alpha + Un_{j\alpha})\delta_{kk'} & \alpha' = \alpha \\ -te^{ik}\frac{1}{L}\sum_j e^{i(k-k')j} = -te^{ik}\delta_{kk'} & \alpha' = r \text{ and } \alpha = l \\ -te^{-ik'}\frac{1}{L}\sum_j e^{i(k-k')j} = -te^{-ik'}\delta_{kk'} & \alpha' = l \text{ and } \alpha = r \\ -t\frac{1}{L}\sum_j e^{i(k-k')j} = -t\delta_{kk'} & \text{otherwise} \end{cases} \\ &= \begin{cases} \begin{cases} \epsilon_\alpha + Un_{j\alpha} & \alpha' = \alpha \\ -te^{ik} & \alpha' = r \text{ and } \alpha = l \\ -te^{-ik'} & \alpha' = l \text{ and } \alpha = r \\ -t & \text{otherwise} \end{cases} & k' = k \\ 0 & k' \neq k \end{cases}. \end{aligned} \tag{B.20}$$

The last step is to find the eigenvalues of the matrix generated by the matrix elements given by (B.20). For a particular choice of basis ordering, the problem is simplified. Consider the following map $\{|k_p\alpha\rangle\}_{p\alpha} \longmapsto \{\mathbf{e}_s\}_{s=1}^{3L}$, where $\{\mathbf{e}_s\}_{s=1}^{3L}$ is the set of ordered standard basis vectors living in a

$3L$ dimensional space, given by:

$$\begin{array}{lll} |k_1 c\rangle \mapsto \mathbf{e}_1 & |k_1 l\rangle \mapsto \mathbf{e}_2 & |k_1 r\rangle \mapsto \mathbf{e}_3 \\ |k_2 c\rangle \mapsto \mathbf{e}_4 & |k_2 l\rangle \mapsto \mathbf{e}_5 & |k_2 r\rangle \mapsto \mathbf{e}_6 \\ |k_3 c\rangle \mapsto \mathbf{e}_7 & |k_3 l\rangle \mapsto \mathbf{e}_8 & |k_3 r\rangle \mapsto \mathbf{e}_9 \\ \vdots \quad \vdots & \vdots \quad \vdots & \vdots \quad \vdots \\ |k_L c\rangle \mapsto \mathbf{e}_{3L-2} & |k_L l\rangle \mapsto \mathbf{e}_{3L-1} & |k_L r\rangle \mapsto \mathbf{e}_{3L} \end{array} \tag{B.21}$$

Using (B.21), the matrix $\boldsymbol{H}_{\text{HF}}^{\text{ref}}$ representing the HF Hamiltonian $\hat{H}_{\text{HF}}^{\text{ref}}$ in the basis $\{|k_p \alpha\rangle\}_{p\alpha}$ with elements given by (B.20) reads:

$$\boldsymbol{H}_{\text{HF}}^{\text{ref}} = \text{diag}(\boldsymbol{A}_{k_1}, \boldsymbol{A}_{k_2}, \cdots, \boldsymbol{A}_{k_L}) \tag{B.22}$$

where the matrices $\{\boldsymbol{A}_{k_1}, \boldsymbol{A}_{k_2}, \cdots, \boldsymbol{A}_{k_L}\}$ are obtained using:

$$\begin{aligned} \boldsymbol{A}_k &= \begin{pmatrix} D_c & -t & -t \\ -t & D_l & -te^{-ik} \\ -t & -te^{ik} & D_r \end{pmatrix} \\ D_c &= \epsilon_c + U\langle \hat{n}_c \rangle \\ D_l &= \epsilon_l + U\langle \hat{n}_l \rangle \\ D_r &= \epsilon_r + U\langle \hat{n}_r \rangle. \end{aligned} \tag{B.23}$$

The task of finding the eigenvalues of the matrix $\boldsymbol{H}_{\text{HF}}^{\text{ref}}$ (allowed energy values for the Hamiltonian $\hat{H}_{\text{HF}}^{\text{ref}}$) is simplified (at least analytically) by virtue of $\boldsymbol{H}_{\text{HF}}^{\text{ref}}$ being a block-diagonal matrix. The eigenvalues (eigenvectors) of such matrix are simply the eigenvalues (eigenvectors) of each block-matrix combined. That is, the allowed energy values at each allowed value of the wave-vector k are the eigenvalues of the corresponding matrix $\boldsymbol{A}_k$ given by (B.23) which completes the proof. □

A derivation of Statement 3

We start by evaluating the quantity $\left|\langle km|j\alpha\rangle\right|^2$ for a given $k_p = k$, from (2.28) and (B.16), we have:

$$|km\rangle = \sum_{\beta} C_{\beta}^{km}|k\beta\rangle = \frac{1}{\sqrt{L}}\sum_{\beta} C_{\beta}^{km}\sum_{n} e^{ikn}|n\beta\rangle. \tag{B.24}$$

By taking the complex conjugate, it follows that:

$$\langle km| = \frac{1}{\sqrt{L}}\sum_{\beta}\left(C_{\beta}^{km}\right)^{*}\sum_{n} e^{-ikn}\langle n\beta|. \tag{B.25}$$

Multiplying (B.25) by $|j\alpha\rangle$ from the right, we get:

$$\langle km|j\alpha\rangle = \left(\frac{1}{\sqrt{L}}\sum_{\beta n}\left(C_{\beta}^{km}\right)^{*} e^{-ikn}\langle n\beta|\right)|j\alpha\rangle = \frac{1}{\sqrt{L}}\sum_{\beta n}\left(C_{\alpha}^{km}\right)^{*} e^{-ikn}\langle n\beta|j\alpha\rangle. \tag{B.26}$$

By the completeness of the basis $|j\alpha\rangle_{j\alpha}$, the only non-vanishing summation term in (B.26) is the $n = j$ and $\alpha = \beta$ term, that is, (B.26) is reduced to:

$$\langle km|j\alpha\rangle = \frac{1}{\sqrt{L}}\left(C_{\alpha}^{km}\right)^{*} e^{-ikj}. \tag{B.27}$$

Multiplying both sides of (B.27) with the complex conjugate, it follows that:

$$\left|\langle km|j\alpha\rangle\right|^2 = \frac{1}{L}\left|C_{\alpha}^{km}\right|^2. \tag{B.28}$$

Now we wish to calculate the DoS functions $\{f_\alpha(E)\}_\alpha$ within a unit cell with sites $\{l, c, r\}$. The value of $f_\alpha(\xi)$ at $E = \xi$, denotes the number of states available per unit energy for the energy value ξ at site α. This is independent of j (which unit cell) due to the degree of homogeneity of the system by construction. The integral of $f_\alpha(E)$ over all possible energy values, would result in the total number of states available at site α. That is, for the spinless case, we have:

$$\int_{-\infty}^{\infty} f_\alpha(E)dE = 1. \tag{B.29}$$

This is nothing but the fact that the maximum number of electrons occupying one site is 1. In the ground state, the total number of states available coincides with the total number of occupied states. However, the total number of occupied states at site α is the same as the electronic density $\langle\hat{n}_\alpha\rangle$. If we instead change the upper limit of integration to μ, where μ is the chemical potential, we are leaving vacancies in states. Namely, the states where $E > \mu$, which indicates that the system is partially filled. The value of the integration is in general less than one (given that $f_\alpha(E) \geq 0$). In the ground state[2], we start filling the system with electrons in energy states from $E = -\infty$ until

[2]Other than the ground state, we would have $\int_{-\infty}^{\infty} f_\alpha(E)P_\alpha(E)dE$, where $P_\alpha(E)$ is the probability of occupancy.

$E = \mu$, the density is then given by:

$$\langle \hat{n}_\alpha \rangle = \int_{-\infty}^{\mu} f_\alpha(E). \tag{B.30}$$

Now we set to find $f_\alpha(E)$. We need to find the expectation value of $\delta(E - \hat{H}_{\text{HF}}^{\text{ref}})$ in the basis $\{|j\alpha\rangle\}_{j\alpha}$, that is:

$$f_\alpha(E) = \langle j\alpha|\delta(E - \hat{H}_{\text{HF}}^{\text{ref}})|j\alpha\rangle. \tag{B.31}$$

Note that due to the completeness of $\{|k_p m\rangle\}_{pm}$, we can make use of the closure relation given by:

$$\sum_{pm} |k_p m\rangle \langle k_p m| = \mathbb{1}. \tag{B.32}$$

From (B.31) and (B.32), we get:

$$\begin{aligned} f_\alpha(E) = \langle j\alpha|\delta(E - \hat{H}_{\text{HF}}^{\text{ref}})|j\alpha\rangle &= \sum_{pm} \langle j\alpha|k_p m\rangle \delta(E - E_{k_p m}) \langle k_p m_{k_p}|j\alpha\rangle \\ &= \sum_{pm} \left|\langle j\alpha|k_p m\rangle\right|^2 \delta(E - E_{k_p m}) \\ &= \frac{1}{L} \sum_{pm} \left|C_\alpha^{k_p m}\right|^2 \delta(E - E_{k_p m}) \end{aligned} \tag{B.33}$$

where we have used (B.28) in the last equality. □

Appendix C

Further Results: DoS

Figure C.1 shows a case of a system described by the energy shifts $\epsilon_c = 0$, $\epsilon_l = -2$ and $\epsilon_r = 3$. All other parameters of the system under study are in accordance with what we presented in Chapter 3. The non-symmetric set $\{\epsilon_\alpha\}_\alpha$ of said system reflects no symmetry on the corresponding DoS functions $\{f_\alpha(E)\}_\alpha$. Other than the special symmetry attained in the system described in Figure 3.1, the discussion is not changed. However, the system considered in Figure C.1 does shed light on the final remark we gave regarding the relationship between U and $\langle \hat{n}_\alpha \rangle$.

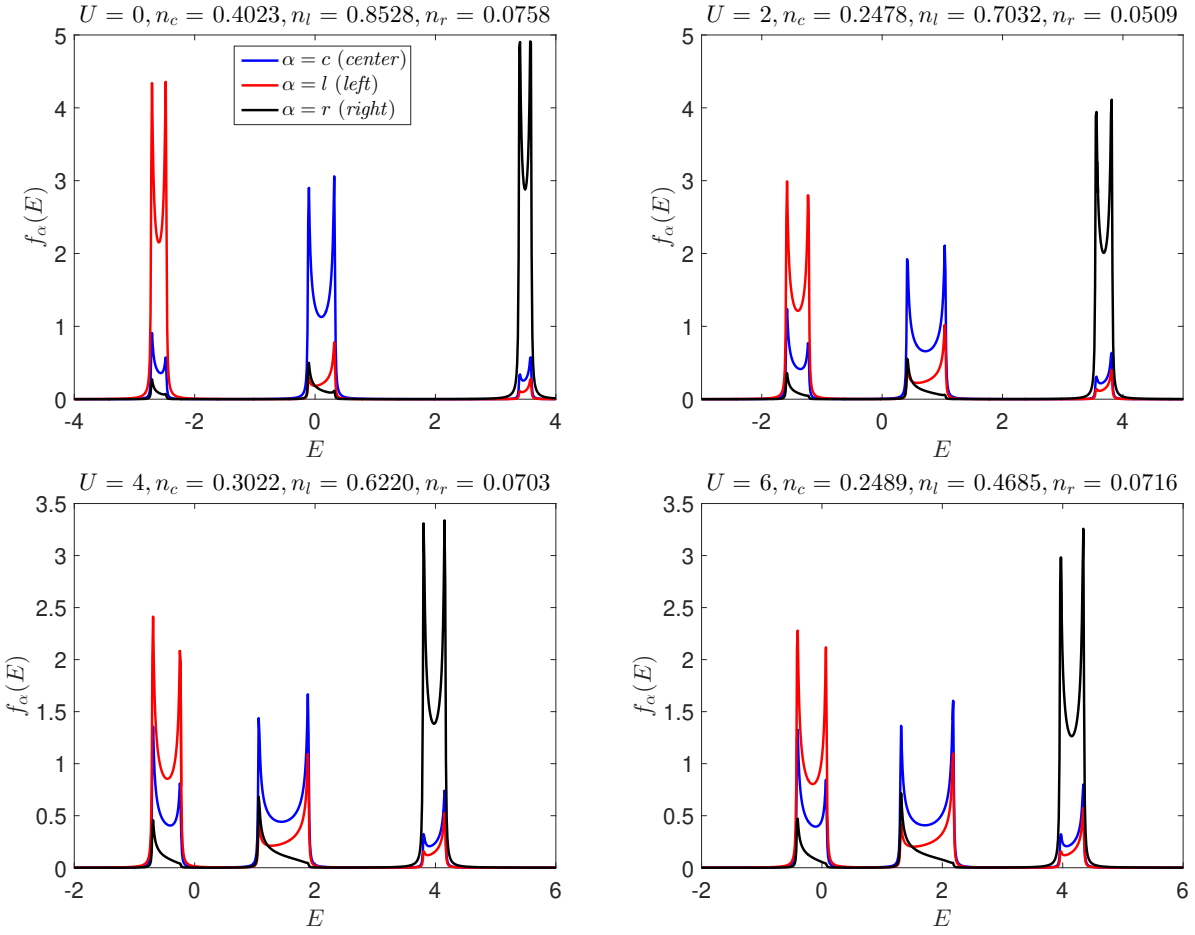

Figure C.1: Comparison between the density of states functions $\{f_\alpha(E)\}_\alpha$ at four different values of the interaction parameter U, for $\epsilon_c = 0$, $\epsilon_l = -2$ and $\epsilon_r = 3$. Left upper panel: $U = 0$, Right upper panel: $U = 2$, Left lower panel: $U = 4$, Right lower panel: $U = 6$. The densities $\{\langle \hat{n}_\alpha \rangle\}_\alpha$ are also displayed for each case. Note the lost symmetry around ϵ_c' compared to Figure 3.1.

Both systems presented in Figure 3.1 and Figure C.1 indicate that the total density within one unit cell $\langle \hat{n}_{\text{cell}} \rangle$ decreases as U increases, which is in agreement with intuition as mentioned previously. However, for a given site density $\langle \hat{n}_\alpha \rangle$, the statement does not hold. Figure C.1 shows an increase in both $\langle \hat{n}_c \rangle$ and $\langle \hat{n}_r \rangle$ when U increased from 2 (Right upper panel) to 4 (Left lower panel), followed

by a slight increase in $\langle \hat{n}_r \rangle$ only, when U increased from 4 to 6 (Right lower panel). We notice that this increase in the density occurred when $\langle \hat{n}_\alpha \rangle$ was relatively small and can be traced back to the effect of the interaction on the range of energy values in which $f_\alpha(E)$ is non-zero. The introduced interaction does indeed make the system accommodate less electrons, however, it does create in some cases enough diversity in the occurring energy values that results in populating vacancies at low density sites. In other words, for a small $\langle \hat{n}_\alpha \rangle$, if the interaction parameter U is high enough, the effect of the diversity in the energy ranges in which the area under $f_\alpha(E)$ is non-zero will win over the shift to the right in $f_\alpha(E)$ due to the repulsive interaction.

Figure C.2 shows the DoS functions for a system described by the energy shifts $\epsilon_c = 0$, $\epsilon_l = -0.1$ and $\epsilon_r = 0.1$ at different values of the local interaction parameter U. All other parameters of the system under study are in accordance with what we presented in Chapter 3.

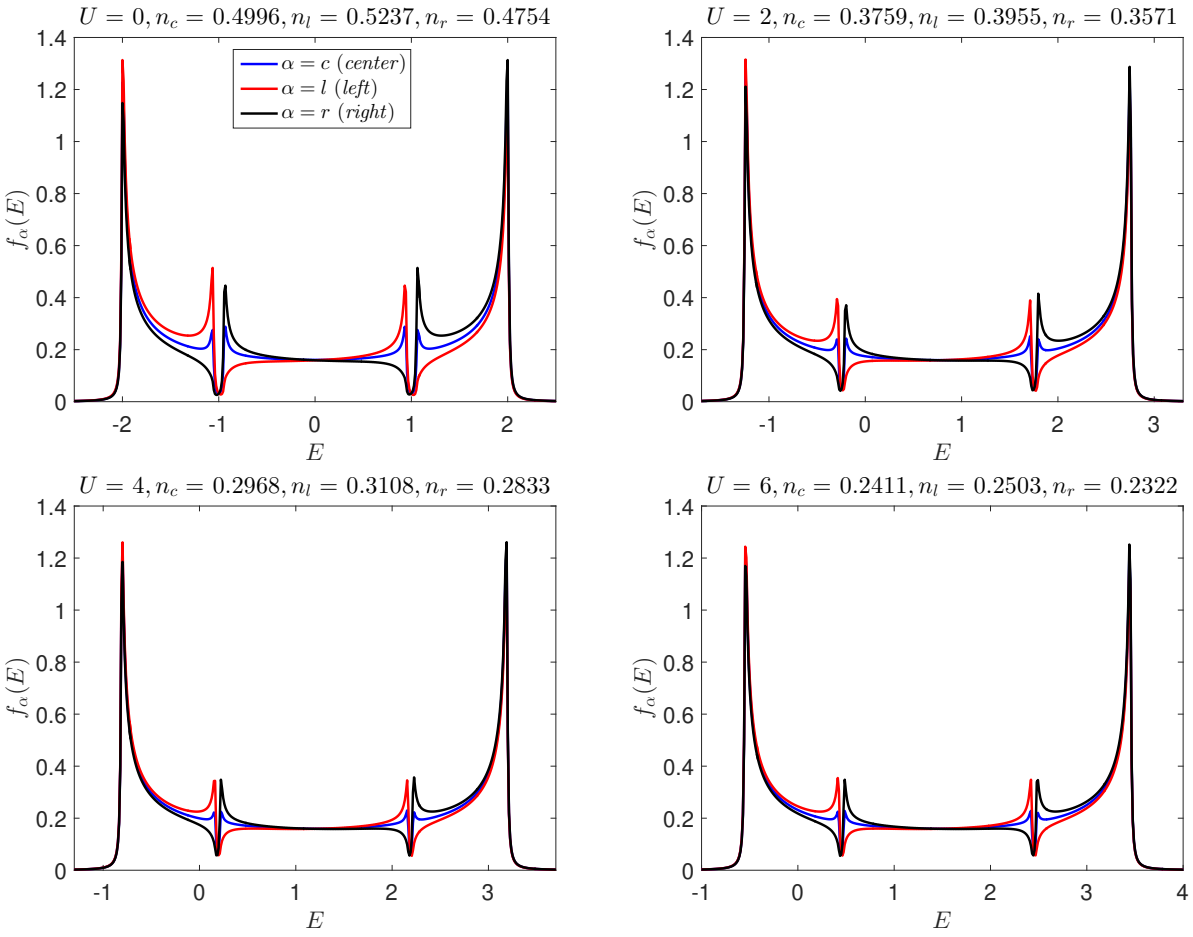

Figure C.2: Comparison between the density of states functions $\{f_\alpha(E)\}_\alpha$ at four different values of the interaction parameter U, for $\epsilon_c = 0$, $\epsilon_l = -0.1$ and $\epsilon_r = 0.1$. Left upper panel: $U = 0$, Right upper panel: $U = 2$, Left lower panel: $U = 4$, Right lower panel: $U = 6$. The densities $\{\langle \hat{n}_\alpha \rangle\}_\alpha$ are also displayed for each case.

Note that due to the energy shifts $\{\epsilon_\alpha\}_\alpha$ being small in magnitude, the DoS functions are interwind in intervals where they are non-zero as opposed to all other systems considered in this thesis where

the shifts $\{\epsilon_\alpha\}_\alpha$ are relatively large. It is also worth noting that as the local interaction parameter U becomes bigger, the DoS functions approach the limit of $\epsilon'_\alpha = U\langle\hat{n}\rangle \ \forall\alpha \in \{l, c, r\}$ where $\langle\hat{n}\rangle$ here is uniform.